Springback Prediction of 7075 Aluminum Alloy V-shaped Parts in Cold and Hot Stamping

Jing Zhou (jingzhou@ustb.edu.cn)
School of Mechanical Engineering, University of Science and Technology Beijing, Beijing 100083, China
Xiaoming Yang
School of Mechanical Engineering, University of Science and Technology Beijing, Beijing 100083, China
Baoyu Wang
School of Mechanical Engineering, University of Science and Technology Beijing, Beijing 100083, China
Wenchao Xiao
School of Engineering and Technology, China University of Geosciences (Beijing), Beijing 100083, China

Research Article

Keywords: Springback, Aluminum alloy, FE model, Analytical model, Stamping

Posted Date: March 19th, 2021

DOI: https://doi.org/10.21203/rs.3.rs-322846/v1

Version of Record: A version of this preprint was published at The International Journal of Advanced Manufacturing Technology on October 28th, 2021. See the published version at https://doi.org/10.1007/s00170-021-08204-x.

Springback prediction of 7075 aluminum alloy V-shaped parts in cold and hot stamping

Jing Zhou[1,2], Xiaoming Yang[1], Baoyu Wang[1,2], Wenchao Xiao[3]

1. School of Mechanical Engineering, University of Science and Technology Beijing, Beijing 100083, China

2. Beijing Key Laboratory of Metal Lightweight Forming Manufacturing, Beijing 100083, China

3. School of Engineering and Technology, China University of Geosciences (Beijing), Beijing 100083, China

*Corresponding author: Jing Zhou

E-mail address: jingzhou@ustb.edu.cn (Jing Zhou)

Abstract

In this paper, the springback behavior of high strength aluminum alloy 7075 is studied by experiments and finite element (FE) simulation. Firstly, an analytical model is established to predict the springback angles and analyze the springback trend. The springback experimental tests are conducted by using the V-shaped stamping dies. The influence of deformation temperature, punch radius and blank holder force on the springback angles are studied. Finally, An FE simulation model is performed to investigate the deformation characteristics and springback process of the aluminum alloy sheet. The results show that the change of springback angles is direct proportional to the punch radius. The springback angles increase with the decreasing deformation temperature and the increasing blank holder force. The stress relaxation that occurs during the die holding stage is the primary reason of reducing the springback compared with cold stamping. Low blank holder force will cause side wall curl, which results in the deviation of forming size. The FE simulation model considering stress relaxation is capable of precisely predicting the change of springback angles, and the simulation results exhibit good consistency with the experimental results.

Keywords: Springback, Aluminum alloy, FE model, Analytical model, Stamping

1. Introduction

The aluminum alloy 7075 as the lightweight material has been widely used in the automotive and aerospace industry [1, 2]. However, AA7075 sheet is difficult to form the complex component at room temperature due to its poor formability [3]. The excellent formability of the aluminum alloy sheet can be obtained by elevating deformation temperature.

The hot stamping and cold die quenching process (or called HFQ process) [4, 5] was invented to improve the formability of aluminum alloy sheets. The improved formability makes it possible to form complex parts in a single work step with the help of rising deformation temperature. The HFQf process which has its great advantages in formability, saving cost and improving productivity has been widely used in automotive industry [6]. At present, the research on the aluminum alloy hot stamping and cold die quenching process is focused on the formability of 5xxx [7] and 6xxx [8] aluminum alloys. The investigations about sheet springback in the high strength aluminum alloy hot stamping process are rarely reported in the published articles. There are a few studies about the springback under the hot stamping condition. Springback is a serious dimensional deviation of the parts after unloading, which reducing the quality of the formed parts [9]. Springback is an intricate problem and related to the whole deformation and heat treatment process. The springback can be significantly reduced by using HFQ process. However, the slight springback of the hot-formed parts still exists after unloading.

Nowadays, many researchers have studied the influence of forming parameters on springback in the forming process. The springback reduction is strongly affected by the die parameters [10, 11]. Su et al. [12] studied the influence of blank holder force on springback. The results show that increasing the blank holder force can reduce springback due to the change of stress state in the deformation region. However, the value of blank holder force cannot be too large in order to control springback, which will cause the forming defects such as thinning and fracture. Zong et al. [13] studied the influence of temperature, punch radius and holding time on springback. The results indicate that the holding time is an extremely important parameter in the hot stamping process. Ma et al. [14] studied the influence of a series of parameters on the V-shaped part springback in the hot stamping process. The springback decreases obviously with the increasing deformation temperature. Wang et al. [15] analyzed the springback of AA5754 by experiments and FE simulation. It is found that the springback increases as the tangential stress gradient increases.

Springback is an inevitable problem after stamping. The work on predicting springback is crucial and necessary research, which can significantly reduce the product costs and design cycle. Wang et al. [16] proposed a mathematical model to explain and predict the springback in the plane-strain bending process. An analytical model considering the sheet thickness and the neutral layer transferring was proposed by Parsa et al. [17] to predict the springback of the double curved parts. In addition, Xue et al. [18] also proposed an analytical model to predict the springback of double-curvature parts. Leu. [19] predicted the springback-radius of the pure bending process by using an analytical model, in which some process parameters were considered incorporating strength ratio, the strain-hardening exponent and the geometric ratio. The analytical model can only predict the change of springback of simple parts and cannot reflect the influence of deformation history on springback.

There should be important and careful consideration about the Bauschinger effect when someone trying to predict the springback in cold stamping process. Tang et al. [20] established a mixed hardening model considering cyclic behavior and the Bauschinger effect. The springback change of AA6022 was predicted by the hardening model. The results show that the prediction model can accurately describe the change of springback. Meanwhile, the paper points out that it is necessary to consider the Bauschinger effect in the prediction model for the process of predicting the springback of anisotropic sheets. A new hardening model was proposed by Gau et al [21]. It was found that the change of sheet stress is the key to accurately predict the springback. Eggertsen et al. [22] evaluated the prediction ability of four common springback prediction models, which are the isotropic mixed, Armstrong-Frederick, Geng-Wagoner, and Yoshida-Uemori models. The results show that the prediction results of Y-U model have good consistency with the experimental results. The Y-U model [23, 24] describing the Bauschinger effect and work hardening can accurately predict the springback in the cold stamping process, which is a reliable prediction model. A modified Y-U model was proposed by Chatti et al. [25] to predict the springback of U-shaped part. The results show that the combination of Y-U model and non-linear kinematic hardening has nice prediction accuracy. The aluminum alloy sheets are adequately heated and soaked in hot stamping process, and the anisotropic behaviors of the materials can be difficultly observed, so the various phenomena caused by the anisotropy could be negligible when forming at elevated temperatures.

In this paper, the springback of aluminum alloy 7075 was studied by forming a V-

shaped part under the hot and cold stamping conditions. Firstly, the analytical model of springback was established to analyze the influence of parameters on springback. The transferring of the neutral layer was considered in the analytical model. Then, the V-shaped part forming tests were conducted. The influence of deformation temperature, punch radius and blank holder force on springback was discussed. The springback mechanism of aluminum alloy at elevated temperature was analyzed by FE model. The springback was predicted by FE simulation model considering the stress relaxation effect in the hot stamping process.

2. Analytical model

The stress state of bending sheets in the thickness direction can be divided into three types: pure elastic deformation in which the material stress on both sides of the neutral layer is less than the yield stress, elastoplastic deformation in which the stress of partial materials is larger than the yield stress and pure plastic deformation in which all materials enter the plastic deformation region, as shown in Fig.1. The pure plastic deformation is just an ideal state and hardly exists in actual production. After unloading, the plastic deformation will be retained, and the elastic deformation will be restored, which will cause the dimensional deviation of the parts. The blank holder force is usually used in the hot stamping process. Therefore, the neutral layer will transfer to the inner layer due to the tensile force causing by the blank holder force, as shown in Fig.1(d).

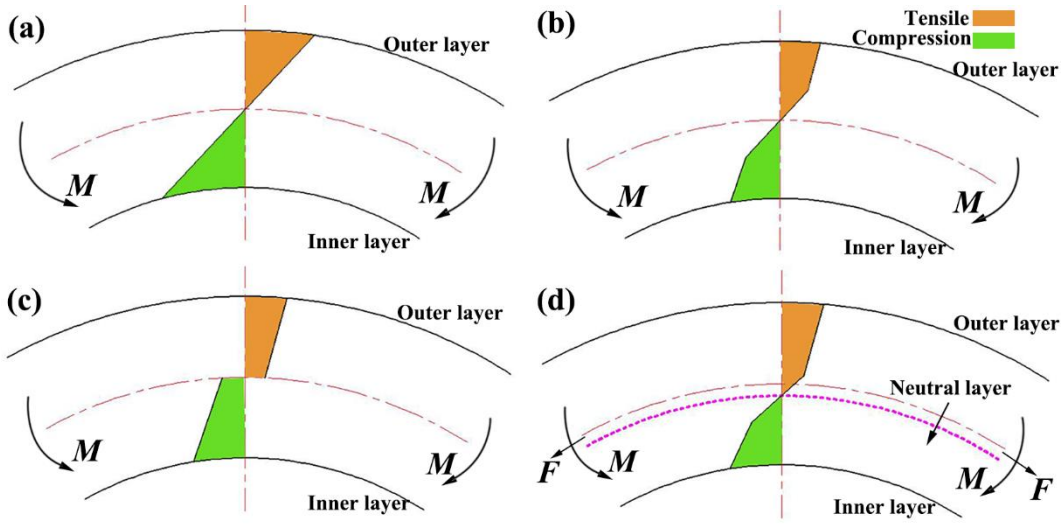

Fig.1 Transverse stress distribution of stretch bending of profile (a) elastic deformation, (b) elastoplastic deformation, (c) pure plastic deformation, and (d) neutral layer transferring

In practical production, the materials on both sides of neutral layer of sheet metal will be kept in the stage of elastic-plastic deformation. The materials of the outer layer

are subjected to tensile stress, and the inner materials are subjected to compressive stress. The springback process of sheet can be considered as the bending moment M is imposed on the sheet along the opposite direction of bending. In order to reduce the complexity of the analytical model, three assumptions are made and itemed as follows:

(1) The material is considered as the rigid-plastic and strain-hardening material. The material complies with the Mises yield criterion.

(2) The deformation process is under plane strain conditions.

(3) The influence of strain rate is negligible. The Bauschinger effect is also negligible.

The influence of elastic recovery on springback can be expressed by bending moment M:

$$M = b\int_{y_T}^{\frac{t}{2}} \bar{\sigma}\left(y - y_T\right)\mathrm{d}y + b\int_{-\frac{t}{2}}^{y_T} \bar{\sigma}\left(y_T - y\right)\mathrm{d}y \tag{1}$$

where y_T is the offset distance of neutral layer; b is the sheet width; t is the thickness of sheet; $\bar{\sigma}$ denotes the equivalent stress, which is the tensile stress caused by friction and plastic deformation. The tensile stress caused by friction can be calculated by $\sigma_F = F/A$, which A is the cross-sectional area of sheet metal and F is the tensile force caused by friction. The tensile force F can be calculated by the following formula [26]:

$$F = \mu F_{\mathrm{h}} \mathrm{e}^{\mu\alpha} \tag{2}$$

where F_{h} is blank holder force, μ is the friction coefficient and α is punch angle.

The circumferential stress should be considered in the analytical model, because the sheet is bending during deformation. The circumferential stress relates to the tensile stress caused by plastic deformation [19, 27], it can be express as:

$$\sigma_\theta = \frac{1+r}{\sqrt{1+2r}}\sigma_x \tag{3}$$

where σ_θ is the circumferential stress, σ_x is the tensile stress caused by plastic deformation, r is the anisotropic value, whose value in this paper is considered equal to 1.

The tensile stress caused by plastic deformation can be expressed as:

$$\sigma_x = K\varepsilon_x^n \tag{4}$$

where K is the temperature dependent constant, n is the strain hardening index, and these two constants can be calculated according to the stress-strain curves. It can be express as:

$$K = 343.35 - 0.6232T \tag{5}$$

$$n = 0.111 - 0.0003T \tag{6}$$

It is assumed that the strain distribution is linear about the neutral layer. The symbol of ε_x denotes the tangential strain, which can be expressed as:

$$\varepsilon_x = \pm \frac{y - y_{\mathrm{T}}}{\rho} \tag{7}$$

where ρ is the curvature radius of neutral layer before springback. The symbol of "±" denotes the stress state, "+" represents tensile stress state and "-" represents compressive stress state.

In conclusion, the bending moment M can be expressed as:

$$\begin{aligned} M &= b\left[\int_{y_{\mathrm{T}}}^{\frac{t}{2}} (\sigma_{\mathrm{F}} + \sigma_\theta)(y - y_{\mathrm{T}})\mathrm{d}y + \int_{-\frac{t}{2}}^{y_{\mathrm{T}}} (\sigma_\theta - \sigma_{\mathrm{F}})(y_{\mathrm{T}} - y)\mathrm{d}y\right] \\ &= b\left[\int_{y_{\mathrm{T}}}^{\frac{t}{2}} \left(\frac{F}{A} + \frac{2\sqrt{3}}{3} K (\frac{y - y_{\mathrm{T}}}{\rho})^n\right)(y - y_{\mathrm{T}})\mathrm{d}y + \int_{-\frac{t}{2}}^{y_{\mathrm{T}}} \left(\frac{2\sqrt{3}}{3} K (\frac{y_{\mathrm{T}} - y}{\rho})^n - \frac{F}{A}\right)(y_{\mathrm{T}} - y)\mathrm{d}y\right] \\ &= \frac{-Fbty_T}{A} + \frac{2\sqrt{3}bK}{3(\mathrm{n}+2)\rho^n}\left[\left(\frac{t}{2} - y_{\mathrm{T}}\right)^{n+2} + \left(\frac{t}{2} + y_{\mathrm{T}}\right)^{n+2}\right] \end{aligned} \tag{8}$$

The springback of curvature can be expressed as follows:

$$\Delta k = \frac{1}{\rho} - \frac{1}{\rho_0} = \frac{M}{EI} = \frac{M}{E\frac{bt^3}{12}} = \frac{-12Fy_T}{Et^2A} + \frac{8\sqrt{3}K}{Et^3\rho^n(n+2)}\left[\left(\frac{t}{2} - y_{\mathrm{T}}\right)^{n+2} + \left(\frac{t}{2} + y_{\mathrm{T}}\right)^{n+2}\right] \tag{9}$$

where ρ_0 is the curvature radius of the neutral layer after springback, I is the moment of inertia, and E is the elastic modulus of the material.

Therefore, the springback-radius ratio can be written as:

$$\frac{\rho}{\rho_0} = 1 - \frac{M\rho}{E\frac{bt^3}{12}} = 1 + \frac{12F\rho y_T}{Et^2A} - \frac{8\sqrt{3}K}{Et^3\rho^n(n+2)}\left[\left(\frac{t}{2} - y_{\mathrm{T}}\right)^{n+2} + \left(\frac{t}{2} + y_{\mathrm{T}}\right)^{n+2}\right] \tag{10}$$

Since the length of neutral layer will not change, the angle after springback can be shown as follows:

$$\alpha_0 = \frac{\alpha\rho}{\rho_0} \tag{11}$$

where α_0 is the angle after springback.

Finally, the angle change due to elastic recovery can be calculated as follows:

$$\Delta\alpha = |\alpha - \alpha_0| = \left|\frac{-12F\alpha\rho y_T}{Et^2A} + \frac{8\sqrt{3}\alpha K}{Et^3\rho^n(n+2)}\left[\left(\frac{t}{2} - y_{\mathrm{T}}\right)^{n+2} + \left(\frac{t}{2} + y_{\mathrm{T}}\right)^{n+2}\right]\right| \tag{12}$$

According to the analytical model, the change of springback angle is influenced

by two types of stress, which are the tensile stress caused by external force and the stress caused by strain hardening. It can be seen from Eq. (12) that the springback angle of parts is mainly related to material strain hardening, sheet thickness, bending angle, die fillet radius and friction. The springback angle is inversely proportional to the elastic modulus and the thickness of sheet, which indicates that the smaller springback can be achieved by increasing the blank thickness and employing the material with large elastic modulus. At the same time, the tensile force should be noticed, which is affected by the friction force. The springback predicted by the Eq.(12) just reflects the change of the elastic recovery, but the equation can hardly explain the springback variation caused by stress release after unloading. The equation can be used to roughly estimate the degree of springback, indicating the trend of springback variation with process parameters changing.

3. Materials and experimental testing

3.1 Materials

The material used in the tests is aluminum alloy 7075-T6 with a thickness of 2 mm, and the chemical composition is shown in Table 1. The yield strength and tensile strength of the sheet is 450 MPa and 540 MPa, respectively.

Table 1. Chemical composition of 7075 aluminum alloy (wt%)

Si	Fe	Cu	Mn	Mg	Cr	Zn	Ti	Al
0.07	0.22	1.4	0.04	2.2	0.19	5.4	0.02	Bal.

3.2 Experimental tests

3.2.1 Hot tensile tests

The hot tensile tests were conducted on a Gleeble-3500 thermal simulation machine to study the flow behavior of aluminum alloy 7075. Aluminum alloy 7075 sheet was cut by wire-electrode cutting, and the length direction is parallel with the rolling direction. The thermal simulation testing procedure is shown in Fig.2(a). The specimens are heated to 455 °C at a heating rate of 20 °C/s. And then, the specimens are heated to the solution temperature at a heating rate of 5 °C/s. The slow heating rate of 5 °C/s is adopted to prevent the specimen overheating. The specimens are soaked for 10 mins to obtain the uniform temperature distribution and homogeneous microstructure. Rapidly cooling is performed to the deformation temperature after constant temperature stage. Finally, the specimens are stretched to fracture, and quenched to room temperature. The hot tensile specimens are deformed at temperatures ranging from 300 °C to 450 °C, and strain rates ranging from 0.01 s^{-1} to 10 s^{-1}.

The hot tensile results are shown in Fig.2(b) and (c). The flow stress of aluminum

alloy 7075 increases with the increasing strain rate and the decreasing temperature.

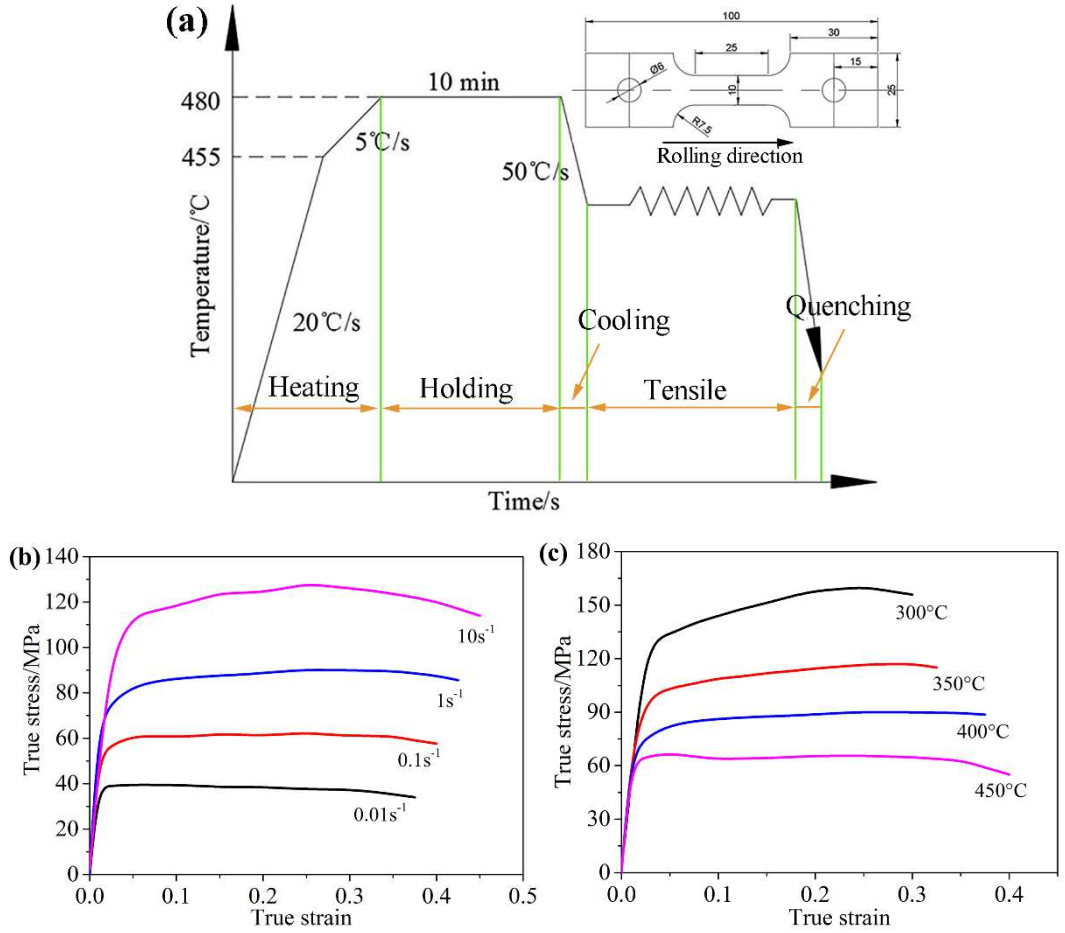

Fig.2 Temperature history of thermal simulation experiments and the obtained true strain-stress curves: (a) temperature history, (b) at deformation temperature of 400 °C, and (c) at strain rate of 1 s^{-1}

3.2.2 V-shaped hot stamping tests

The V-shaped part stamping is conducted to study the springback after unloading. The V-shaped die-set is shown in Fig.3. Before testing, the sheet with a dimension of length 180 mm and width 50 mm is sprayed with a coat of graphite lubricant. During the hot stamping, the sheet is heated to the solution treatment temperature and rapidly cooled to the deformation temperature, and then, the heated sheet is rapidly transferred to the holder. The die driven by a 60-ton press moves to the fixed punch for completing the stamping and quenching, and the whole process lasts about 30 seconds. For the specimen formed at room temperature, the heating is not executed, and the specimen is directly stamped by the dies under the cold stamping condition. The blank holder force is provided by the nitrogen gas spring. After the stamping, the change of feature angles is measured through the mapping of part outline.

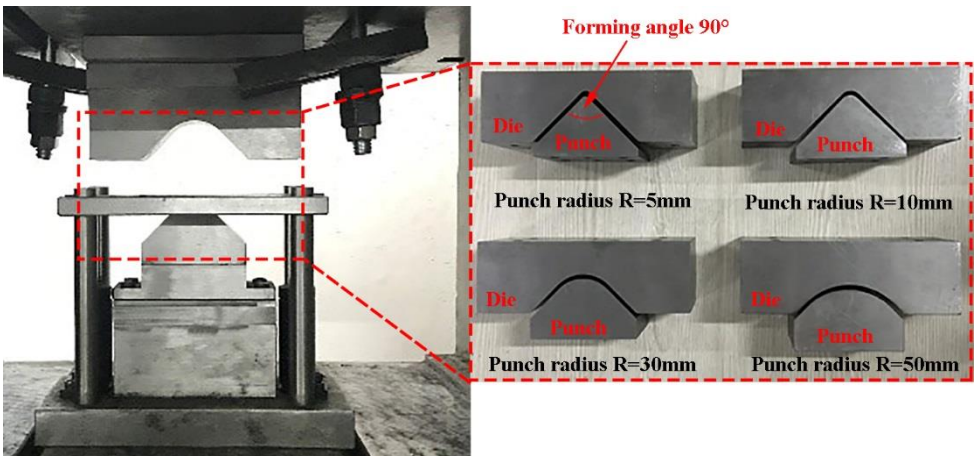

Fig.3 The V-shaped stamping tools

In this paper, the influence of the sheet temperature, punch radius and blank holder force on springback is investigated. The parameters of V-shaped hot stamping are listed in Table 2.

Table 2. Parameters of V-shaped hot stamping

Parameters	Values
Sheet deformation temperature/°C	25, 200, 300, 350, 400
Punch radius/mm	5, 10, 30, 50
Blank holder force/kN	1.7, 3.4, 5, 6.8
Stamping speed/mm/s	20
Forming angle/°	90
Tool temperature/°C	25

To accurately measure the springback angle, the measured specimen with the width of 10 mm is cut from the deformed part. The measured springback angles are shown in Fig.4. The $\Delta\alpha$ of forming region and $\Delta\beta$ of holder region is mainly studied. The following formulae are adopted to calculate the springback angles.

$$\begin{aligned}\Delta\alpha&=\alpha-90^{\circ}/2\\ \Delta\beta&=\beta-135^{\circ}\end{aligned} \tag{13}$$

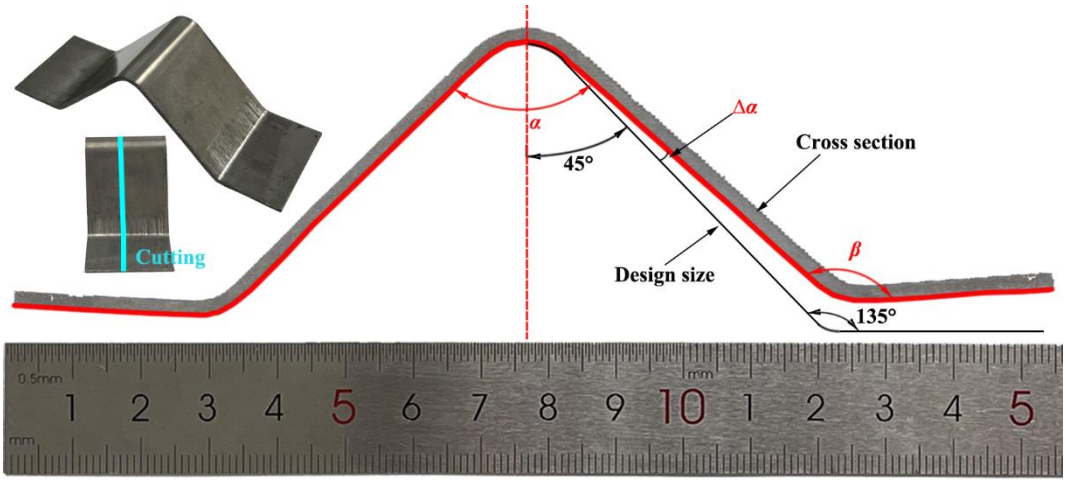

Fig.4 The measurement of the springback angles

4. FE model description

The FE model of V-shaped part is established via the FE software Abaqus to analyze the process of forming and springback, as shown in Fig.5. The model contains four components: die, punch, holder, and blank. The simulation process mainly contains four steps: holding, stamping, quenching and springback. In cold stamping simulation process, the simulation process only contains three steps: holding, stamping and springback. During the simulation, the die moves down to complete the stamping, and the punch is fixed. The blank holder force is applied to the holder during the whole stamping process. The forming tool are removed to simulate the springback phenomenon after stamping. The symmetry plane of sheet is fixed in the springback simulation. An explicit time integration scheme is applied in the simulation of stamping process, and an implicit time integration algorithm is used to compute the springback of formed parts.

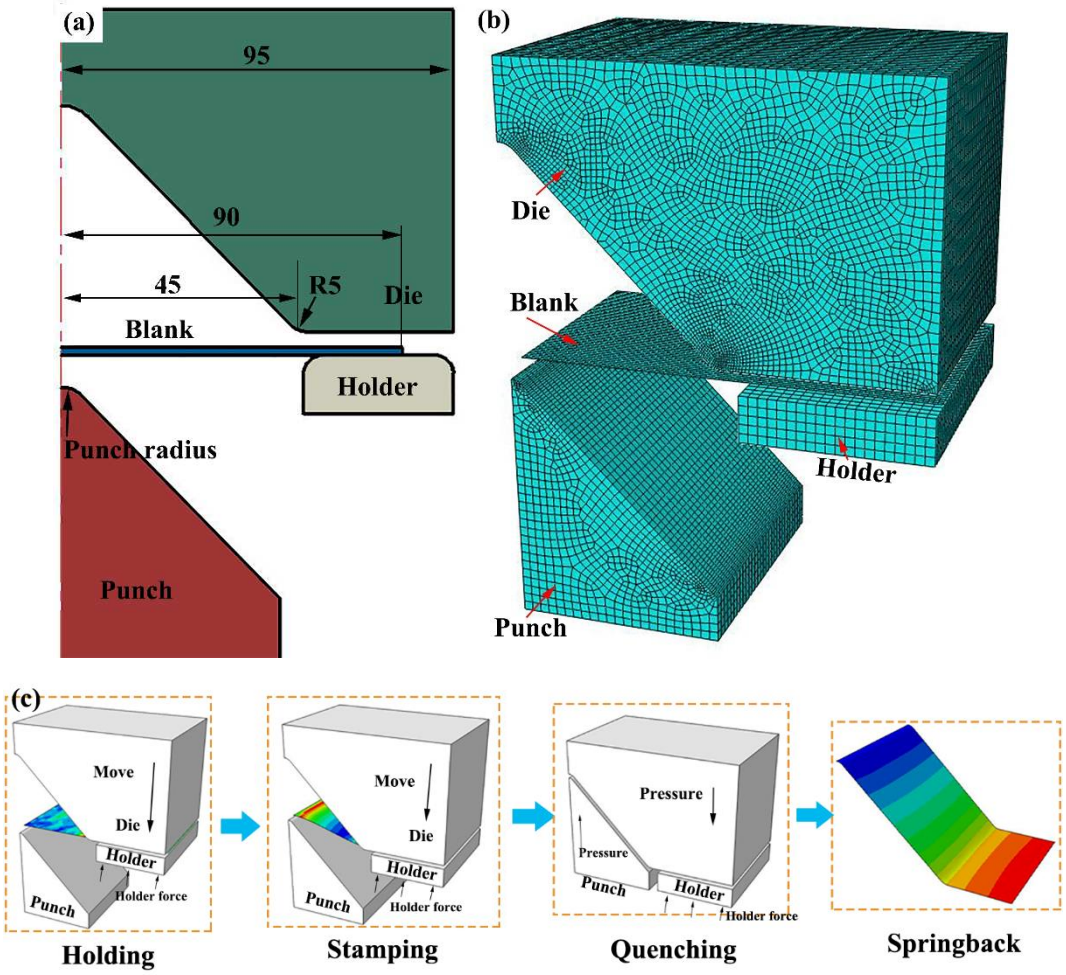

Fig.5 The V-shaped FE model (a) the size of the FE model, (b) the FE model, and (c) the simulation procedure

The tool is set as rigid body, and the element type C3D8T coupled the temperature and displacement is used for the tool. The sheet is meshed by S4RT the shell element coupled the temperature and displacement. The thickness integration points of the sheet is set as 9. The materials of the tool and sheet is set as AISI -H13 and aluminum alloy 7075, respectively. The physical parameters of the tool and sheet are shown in Table 3. During the stamping process, the heat exchange occurs between the hot sheet and cold tool. Therefore, the interfacial heat transfer coefficient (IHTC) measured by Xiao et al. [28] is used in this paper, as shown in Fig.6. The interfacial heat transfer coefficient increases with the increasing of contact pressure. The true stress-strain curves of aluminum alloy 7075 are input into the FE simulation software. The true stress-strain curves below 300 °C reported by Zhang et al. [29] are used in the FE simulation.

Table 3. The thermophysical parameters of the tool and sheet material

Parameters		Values				
Temperature(°C)		20	100	200	300	400
Specific heat(J/kg • K)	H13	460	-	510	-	548
	7075	840	910	972	1018	1128
Thermal conductivity(W/m • K)	H13	24.4	-	29.2	-	29.9
	7075	13	52	91	121	143

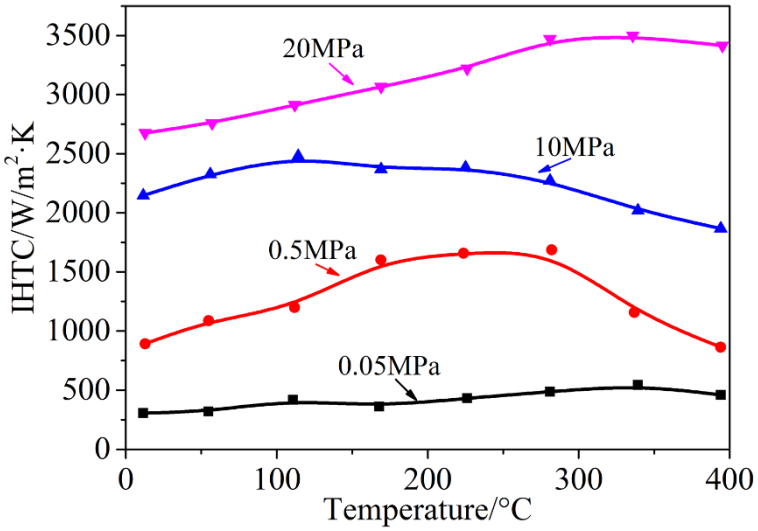

Fig.6 Interfacial heat transfer coefficient of the AA7075 and H13 steel contact pair

5. Results and discussion

5.1 The V-shaped hot stamping results

The intact formed parts after stamping are shown in Fig.7. The sheet has been formed at cold and hot stamping conditions. However, the formed parts exhibit different degrees of springback. The V-shaped part has large springback angle when the forming temperature is 25 °C. The springback defects has been alleviated by using the hot stamping process. In addition, it can be seen from Fig.7 that the length of the side wall

decreases with the increasing punch radius. It manifests that the springback of forming angle α has a great influence on the angle β at a large punch radius.

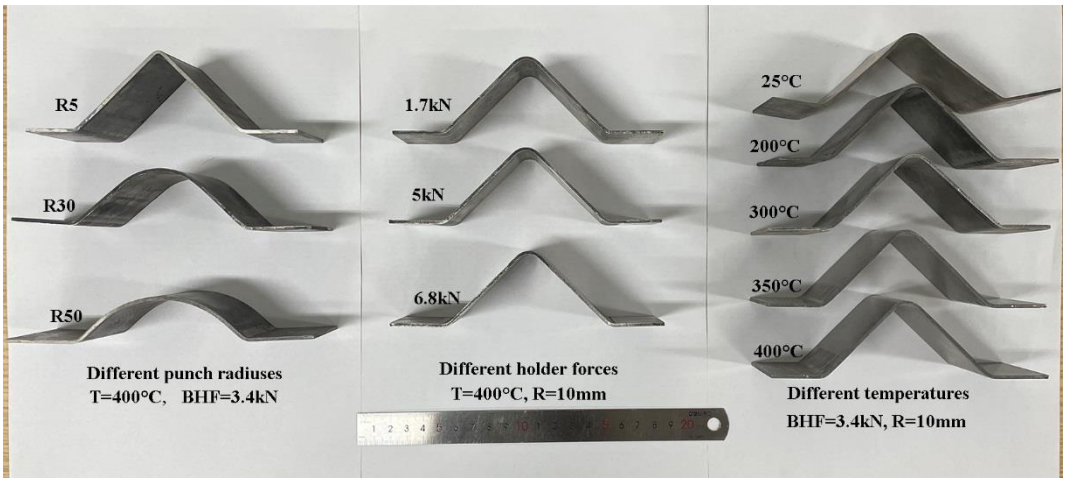

Fig.7 The formed parts at different parameters

The change trend of springback can be calculated by the analytical model. The effect of parameters on springback is shown in Fig.8. The springback angle increases with the increasing forming angle. The main reason is that the smaller length of the deformation zone can be obtained at the larger forming angle. It can be seen from Fig.8(a) that the forming zone length decreases from O_1A_1 to O_5A_5 when the forming angle increases from 30° to 150°. As a result, the proportion of the elastic deformation zone in the sheet metal is increased, and then the springback angle increases. The springback angle decreases with the increasing neutral layer transferring. The increasing of neutral layer transferring leads to the increasing of metal plastic deformation. The change of angle β is related to the deformation history. It is difficult to predict the specific angle value by using the analytical model. Therefore, the springback-radius ratio of angle β is predicted by the analytical model. It can be seen from Fig.8(c) that the springback-radius ratio increases with the increasing deformation temperature. The springback will be eliminated when the springback-radius ratio equals 1.

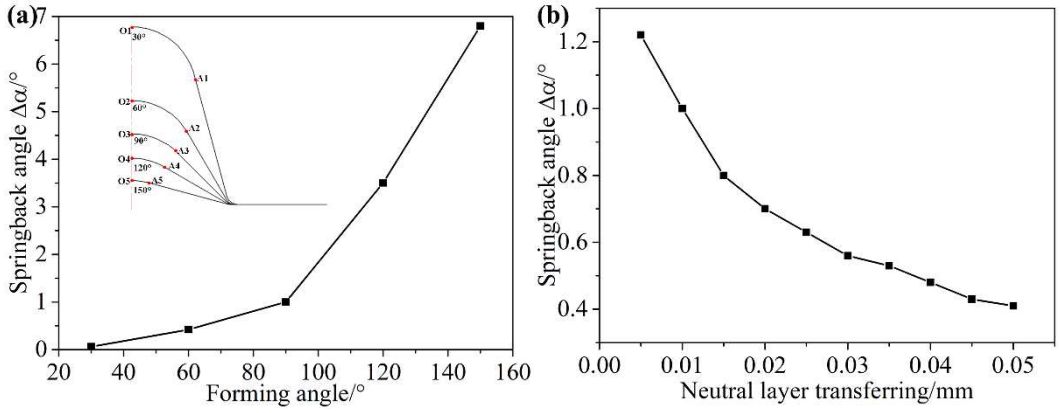

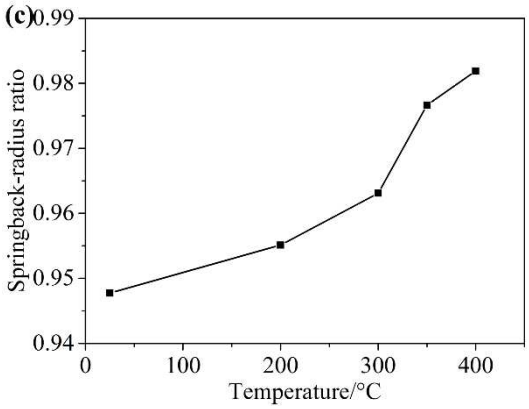

Fig.8 The effect of process parameter on springback (a) forming angle, (b) neutral layer transferring, and (c) the change of springback-radius ratio for angle β

5.2 Influence of temperature on springback

The sheet temperature distribution was recorded by an infrared thermal camera during the tests. The sheet temperature distribution is shown in Fig.9 after holding step. It can be seen that the temperature distribution obtained from the FE simulation show good consistency with the experimental results. The maximum sheet temperature, captured by the infrared thermal camera, drops from 450 ° C to 385 ° C after holding in the experimental tests. And the maximum sheet temperature after holding is about 364 ° C in the simulation results. The sheet temperature of holding region rapidly decreases due to the heat exchange between the blank holder and sheet. The springback appears after unloading caused by the inhomogeneous temperature distribution of sheet.

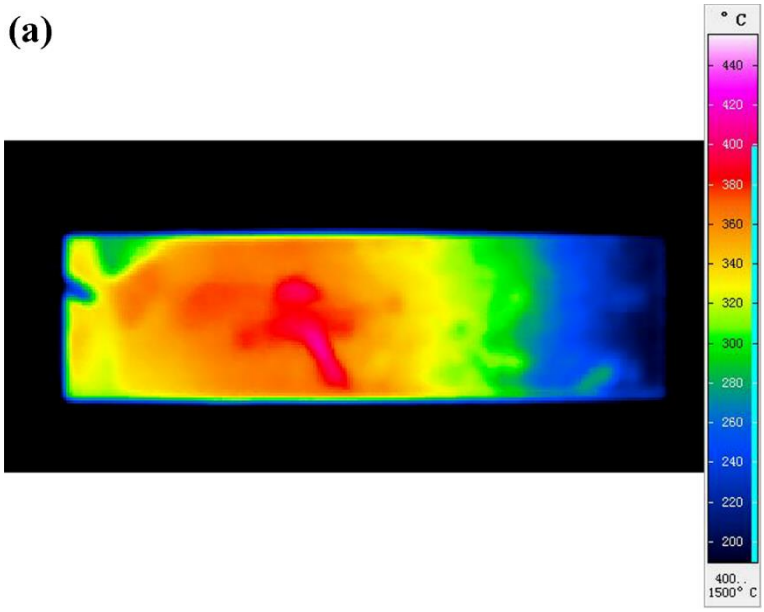

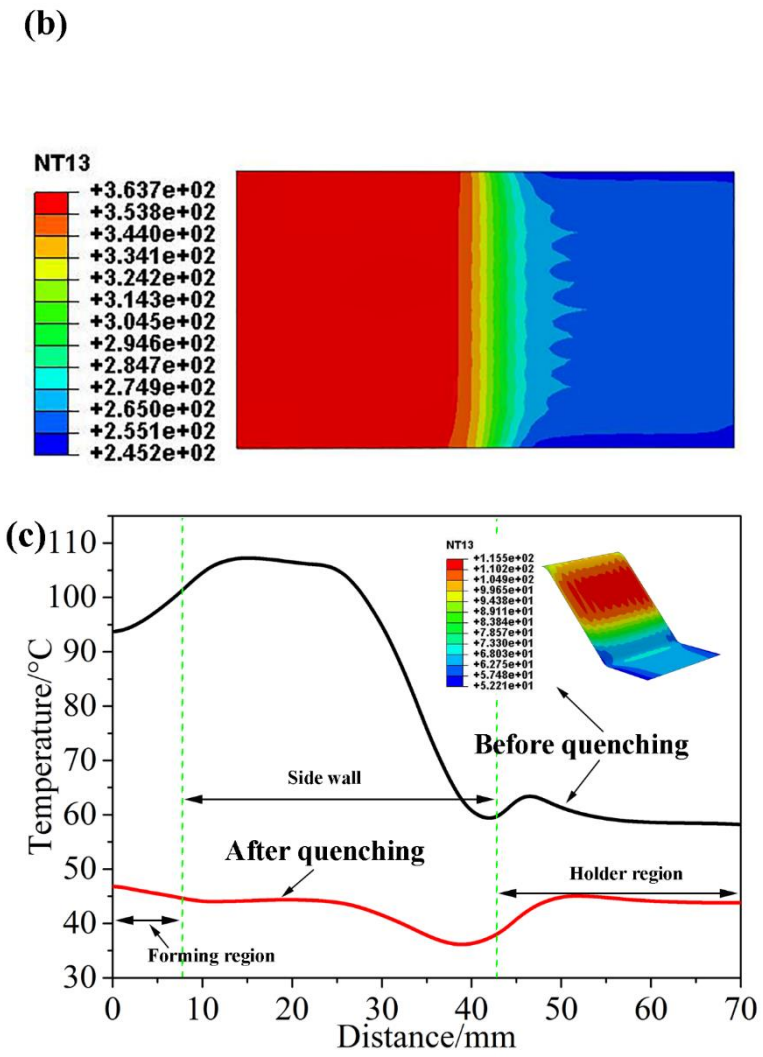

Fig.9 The temperature distribution of sheet (a) experimental result after holding, (b) simulation result after holding, and (c) temperature distribution variation after stamping

The change of springback angles with deformation temperature is shown in Fig.10 when the punch radius is 10 mm and the blank holder force is 3.4 kN. The analytical model only considering the effect of elastic recovery has poor ability to predict the springback of sheet metal at high temperature. The springback angles decrease with the increasing sheet temperature. The springback angle decreases rapidly at the temperature ranging from 25 °C to 300 °C, and $\Delta\alpha$ decreases by 4.2°. The springback angle reduces slowly from the temperature of 300 °C to 400 °C, and $\Delta\alpha$ only decreases by 0.05°. This is because that the elastic modulus and yield strength of the materials decreases obviously when the sheet temperature increases from 25 °C to 300 °C. However, the change of elastic modulus and yield strength is smaller when the temperature increases from 300 °C to 400 °C. In the deformation process, the materials will undergo the elastic deformation stage at first. The plastic deformation will take place in materials when the

deformation force exceeds the yield strength. After unloading, the elastic deformation will recover to the initial stage, while the plastic deformation will remain permanently. At the same deformation degree, there is more elastic deformation remaining in the deformed parts at low temperature. The more elastic deformation will appear in the V-shaped part at low temperature due to the high yield strength. The more plastic deformation will remain in the parts after unloading at high deformation temperature due to the lower yield strength [30]. Therefore, the springback angle decreases with the decreasing yield strength.

By comparing the experimental and simulation results, it can be found that the FE simulation has great prediction accuracy. The FE model established in this paper can accurately predict the trend and value of the springback.

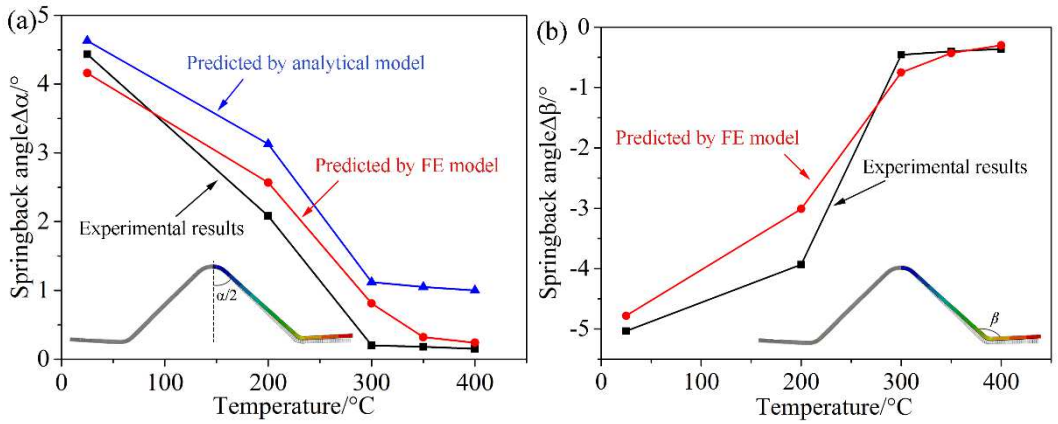

Fig.10 The change of springback angles (a) the change of springback angle $\Delta\alpha$, and (b) the change of springback angle $\Delta\beta$

On the other hand, the reduction of stress is another reason resulting in the springback reduction. The decrease of stress is mainly because of the effect of stress relaxation at high temperature when the stroke is fixed. The stress relaxation is defined as that the stress decreases with the time increasing [31]. The distribution of Mises stress before and after quenching is shown in Fig.11. It can be seen that the Mises stress after stamping is large at 25 °C. The maximum stress appears at the side wall, and the minimum stress appears at the corner (BC segment). However, the region of punch radius (OA segment) has large stress. After springback, the stress of the side wall decreases at 25 °C, while the stress of the corner (BC segment) increases. Moreover, the stress relaxation will not happen at room temperature. Therefore, the reduction of stress in the side wall is caused by the elastic recovery at 25 °C. The elastic recovery is transmitted to the free end. The stress of the corner increases due to the elastic recovery of side wall. The large stress in the corner increases the springback angle. However, the

stress after quenching is almost 0 for the deformation temperature of 400 °C. The change of the stress is obviously because of stress relaxation. In addition, the influence of stress relaxation on the stress reduction is of great significant at high deformation temperature.

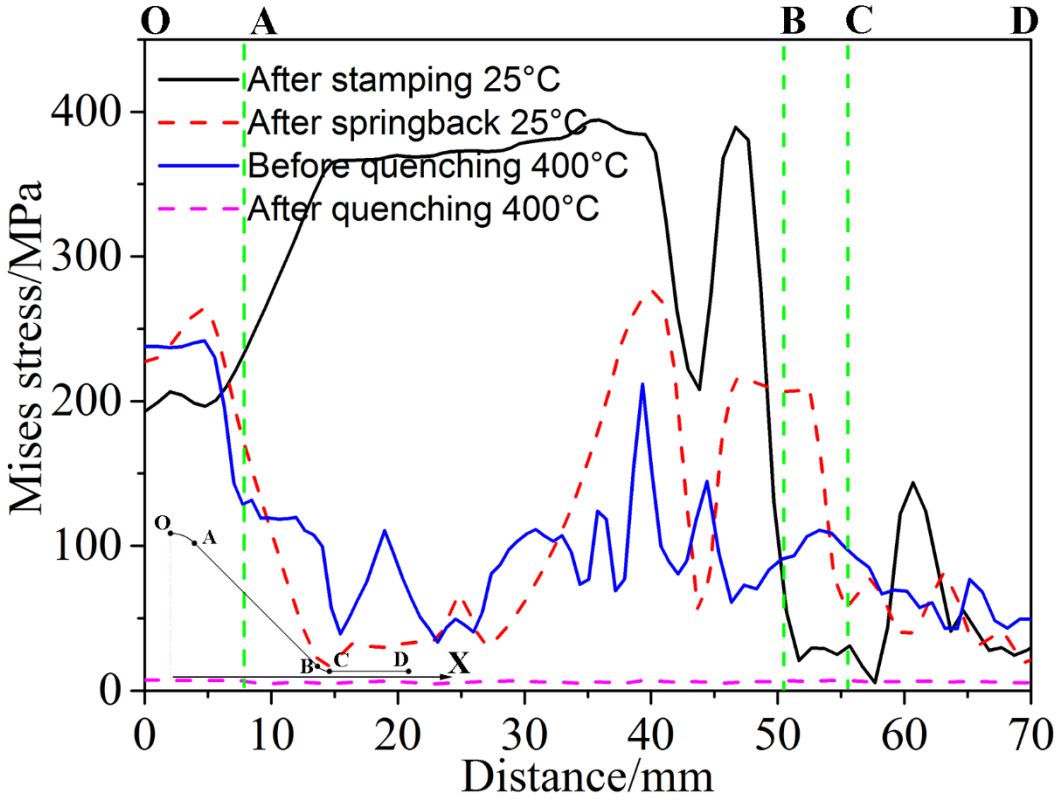

Fig.11 The distribution of Mises stress along a section at different process stages and temperatures

5.3 Influence of punch radius on springback

The influence of punch radius on springback angles is shown in Fig.12 when the deformation temperature is 400 °C and the blank holder force is 3.4 kN. The springback angles increase with the increasing punch radius. The radius of holder region (forming angle β) is set as a constant, so the springback change of angle β is not be predicted by the analytical model. The change trend of the springback angle predicted by Eq. (12) is same as the experimental results. However, the predicted results obtained from FE simulation have greatly consistency with the experimental results, by contrasting them with the results obtained from analytical model. The springback angle $\Delta\alpha$ increases from -0.14° of punch radius 5 mm to 2.52° of punch radius 50 mm. The springback angle $\Delta\beta$ increases from 0.3° of punch radius 5 mm to 2.02° of punch radius 50 mm. The FE model can well predict the springback angles of different punch radius in the stamping tests.

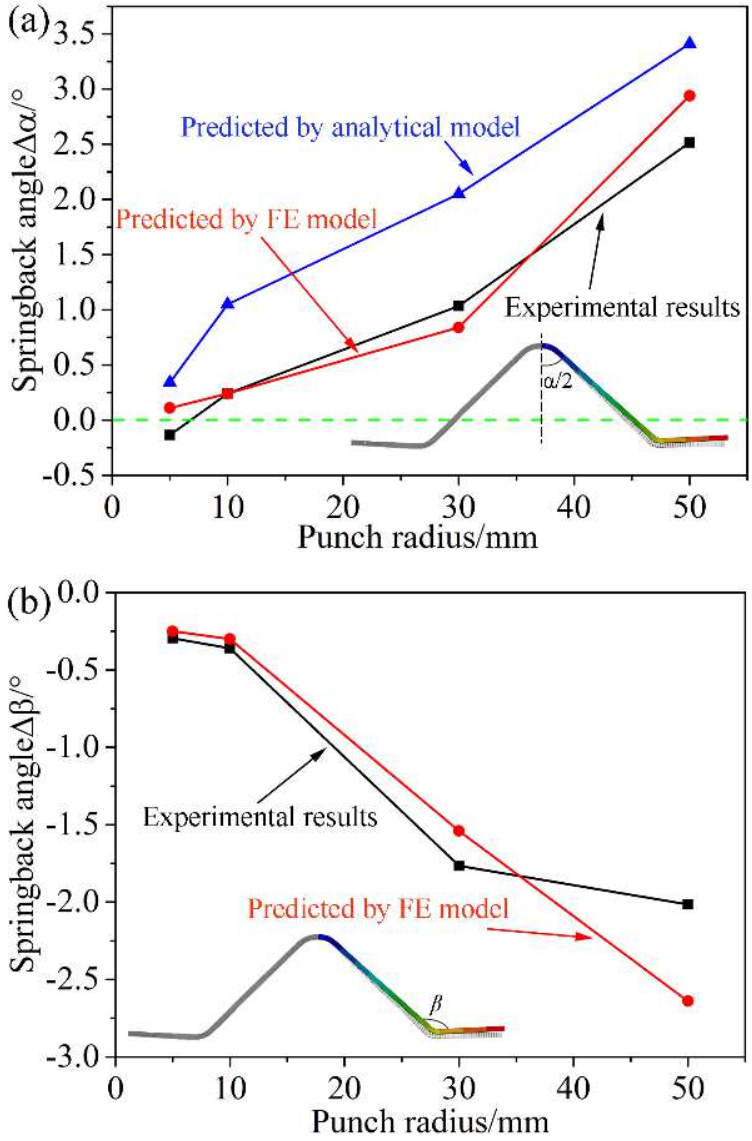

Fig.12 Influence of punch radius on springback angles (a) the change of springback angle $\Delta\alpha$, and (b) the change of springback angle $\Delta\beta$

The change of the Mises stress distribution is shown in Fig.13. The stress releases to a lower level after quenching due to the effect of stress relaxation. It can be seen that the position of maximum stress is different for various punch radiuses. The maximum stress appears at the forming angle region when the punch radius is 5 mm. The maximum stress is found near the holder radius region at punch radius of 50 mm due to the increasing length of bending region. The average stress level of punch radius 5 mm is much larger than that of punch radius 50 mm. Therefore, the change of stress has more distinct effect on the springback when the punch radius is 50 mm, comparing with the punch radius of 5 mm.

As shown in Fig.13, the OA_1 segment represents the forming region of punch radius 50 mm. The change of stress is more complex at forming region with the punch

radius 50 mm due to the longer length of forming region. As a result, the length of side wall decreases with the increasing of forming region. The change of angle α is greatly affected by angle β. The deformation characteristics of the metal sheet near the forming angle β are more likely to disturb the springback of forming angle α. However, the length of forming region is short when the punch radius equals 5 mm resulting in the long side wall. The side wall relieves the effect of stress on springback angle. On the other hand, more elastic deformation accumulates in the forming region at the radius of 50 mm.

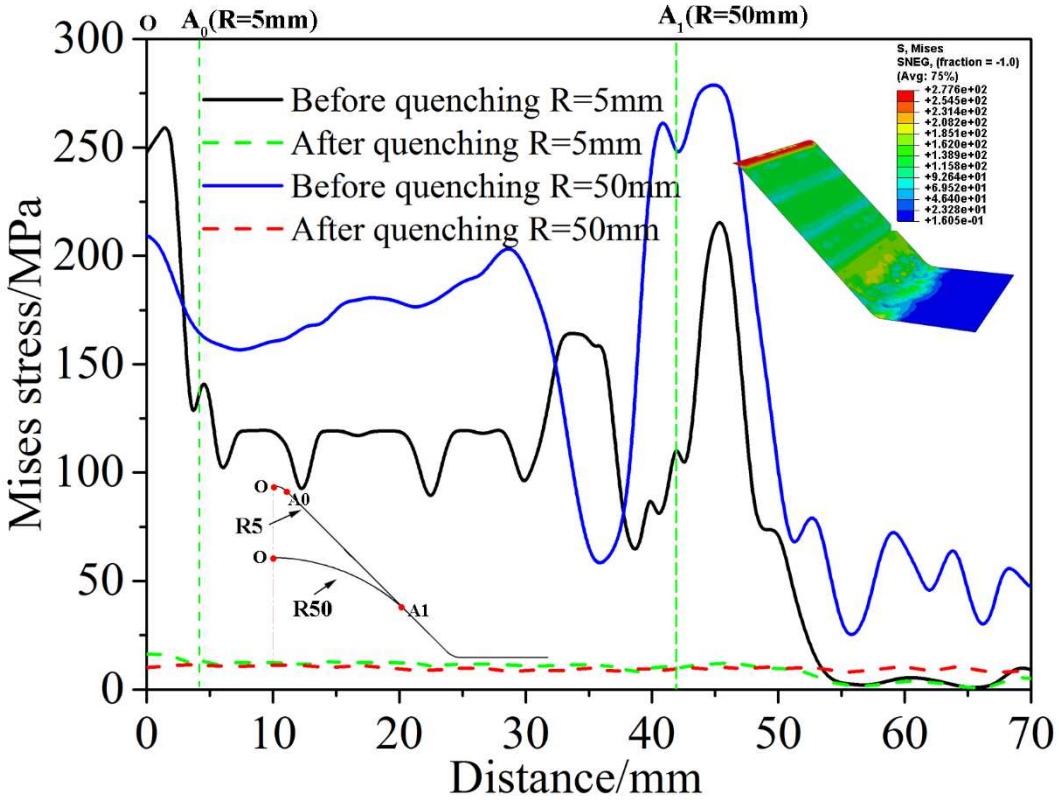

Fig.13 The distribution of Mises stress along a section at different process stages and punch radiuses

5.4 Influence of blank holder force on springback

The change of springback angles with the various blank holder force is shown in Fig.14 when the deformation temperature is 400 °C, and the punch radius is 10 mm. The springback angles present decline trends with the increasing of blank holder force. According to the experimental results, the angle $\Delta\alpha$ decreases from 0.28° of blank holder force 1.7 kN to 0.13° of blank holder force 6.8 kN, down by about half. Comparing with the angle $\Delta\alpha$, the angle $\Delta\beta$ changes obviously which changes from -0.85° to 0.11°, as the blank holder force increases from 1.7 kN to 6.8 kN.

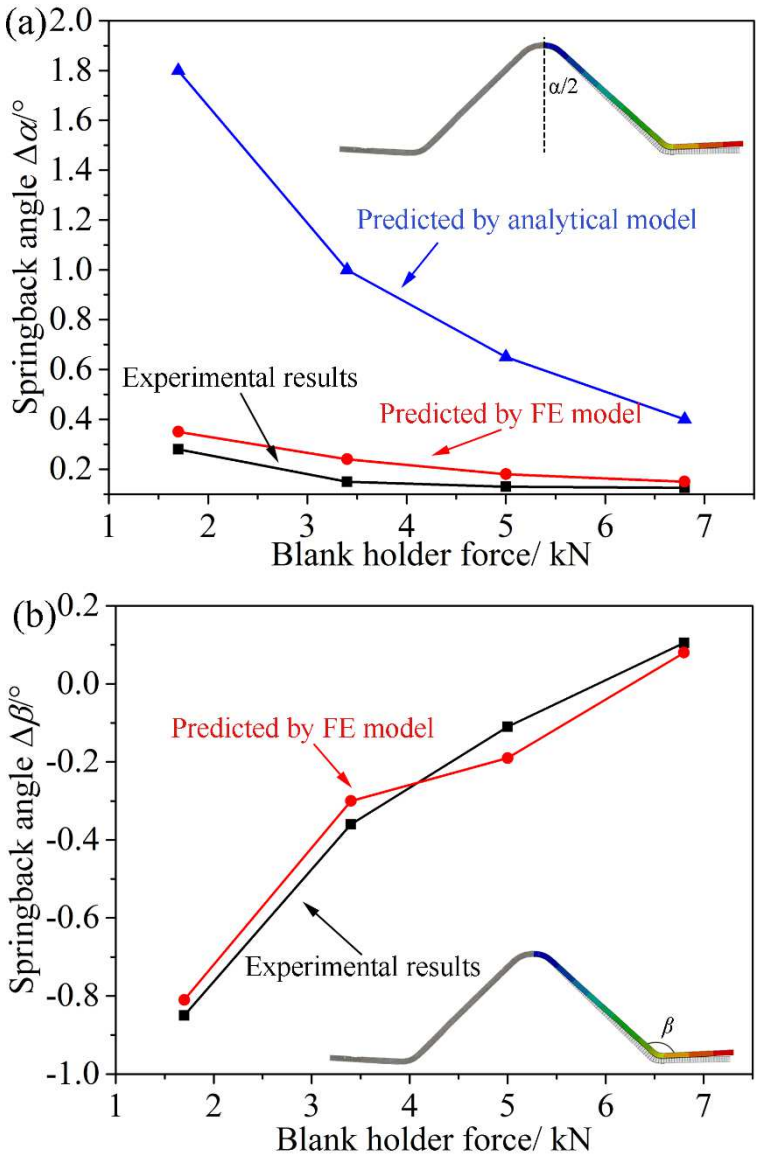

Fig.14 Influence of blank holder force on springback angles (a) the change of springback angle $\Delta\alpha$, and (b) the change of springback angle $\Delta\beta$

As the previous analysis, the neutral layer transfers under the action of the blank holder force. The offset of the neutral layer increases with the increasing blank holder force. Therefore, the more plastic deformation can be reserved in the deformed parts after unloading. The less elastic recovery results in the low springback.

Furthermore, the sheet is deformed at high temperature which reduces the strength of materials. Thus, the curl will occur in the side wall of parts, as shown in Fig.15. It can be seen that the curl of the side wall is large at low blank holder force. However, the curl of the side wall can be suppressed at a large blank holder force. The curl will be stretched and compressed at the end of stamping stage resulting in the stress concentration of the forming angle β. The complex stress near the forming angle increases the springback angles. Under the action of large blank holder force, the sheet

in the forming process sustains the tensile state. The larger blank holder force can obtain the smaller curl of the side wall which leading to a low springback. The deviation of the part obtained from the simulation is shown in Fig.15(c). The maximum deviation is 0.6mm due to the curl. According to the experimental result, the curl also can be observed at the side wall.

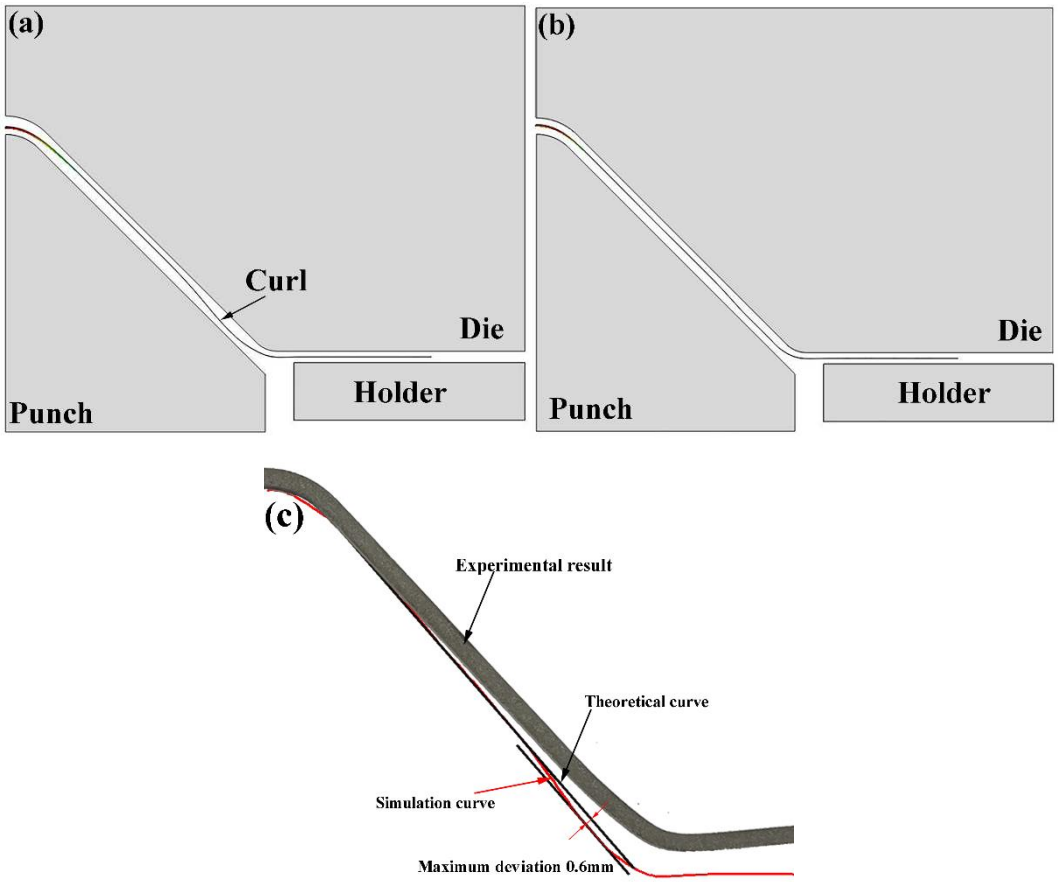

Fig.15 The curl of side wall at different blank holder forces (a) blank holder force 1.7 kN, (b) blank holder force 6.8 kN, and (c) deviation causing by curl

6. Conclusions

In this paper, the analytical model of sheet springback was established to analyze the change of springback. The effects of experimental parameters on springback were approximately analyzed by the analytical model, and the V-shaped stamping experiments were conducted. The FE simulation considering stress relaxation was built and carried out to analyze the deformation characteristics and the springback of V-shaped parts. The influences of temperature, punch radius, and blank holder force on springback were discussed. The conclusions are drawn as follows:

(1) According to the analytical model, the change of springback angle is influenced by two kinds of stress, which are the tensile stress caused by external force and the stress caused by strain hardening. The springback angle of parts is mainly related to

material properties, sheet thickness, forming angle, punch radius, and friction.

(2) The springback angles decreases with the increasing deformation temperature. The springback angle $\Delta\alpha$ decreases from 4.4° at 25 °C to 0.15° at 400 °C, decreasing by 96.5%. The stress relaxation is the principal mechanism of the springback reduction for the hot stamping process of aluminum alloy. The elastic recovery is the main reason resulting in the change of forming angle under the cold stamping condition.

(3) The springback angles increases with the increasing punch radius due to the increasing length of the forming region. The springback angle $\Delta\alpha$ increases from -0.14° to 2.52° when the punch radius increases from 5 mm to 50 mm. The springback angle $\Delta\beta$ increases from 0.3° at the punch radius of 5 mm to 2.02° at the punch radius of 50 mm. The elastic deformation of aluminum alloy sheets has been accumulated in the large punch radius resulting in the large springback.

(4) The small blank holder force could scarcely provide enough tensile force for suppressing the side wall curl, which makes the crooked profile appearing in the side wall during hot stamping process. Therefore, the change of springback angles show an increasing trend with the decreasing of the blank holder force. The angle $\Delta\alpha$ decreases by 0.15° when the blank holder force increases from 1.7 kN to 6.8 kN. The angle $\Delta\beta$ changes obviously which changes from -0.85° to 0.11°, as the blank holder force increases from 1.7 kN to 6.8 kN.

Declarations

Funding: This work was supported by the Joint Funds of the National Natural Science Foundation of China (Grant number U51705018). This work was also supported by the Beijing Laboratory of Modern Transportation Metal Materials and Processing Technology. This work was also supported by Beijing Key Laboratory of Metal Forming Lightweight.

Conflicts of interest/Competing interests: All the authors declare that they have no conflicts of interest.

Availability of data and material: The datasets are available from the corresponding author on reasonable request.

Code availability: Not applicable.

Authors' contributions:

Jing Zhou: methodology, modelling, overseeing analysis, writing original draft.
Xiaoming Yang: methodology, testing, data collection and analysis, modelling

Baoyu Wang: writing review & editing, resources
Wenchao Xiao: testing, writing review & editing

Ethics approval: Not applicable.

Consent to participate: All the authors listed have approved to participate the study.

Consent for publication: All the authors listed have approved the manuscript to publish.

References

[1] Muraoka Y, Miyaoka H (1993) Development of an all-aluminum automotive body. J Mater Process Technol 38: 655-674. https://doi.org/10.1016/0924-0136(93)90042-5

[2] Zhang CS, Yang S, Wang CX, Zhao GQ, Gao AJ, Wang LJ (2016) Numerical and experimental investigation on thermo-mechanical behavior during transient extrusion process of high-strength 7xxx aluminum alloy profile. Int J Adv Manuf Technol 85: 1915-1926. https://doi.org/10.1007/s00170-016-8595-3

[3] Liu LJ, Liu ZX, Zhang ZQ (2019) Investigation on strengthening of 7075 aluminum alloy sheet in a new hot stamping process with pre-cooling. Int J Adv Manuf Technol 103: 4739-4746. https://doi.org/10.1007/s00170-019-03890-0

[4] Foster A, Dean TA, Lin JG (2013) Process for forming aluminum alloy sheet components. European Patent EP2324137 A1.

[5] Garrett RP, Lin JG, Dean TA (2005) An investigation of the effects of solution heat treatment on mechanical properties for AA6xxx alloys: experimentation and modelling. Int J Plast 21: 1640-1657. https://doi.org/10.1016/j.ijplas.2004.11.002

[6] Zheng KL, Zhu L, Lin JG, Dean TA, Li N (2019) An experimental investigation of the drawability of AA6082 sheet under different elevated temperature forming processes. J Mater Process Technol 273: 116225. https://doi.org/10.1016/j.jmatprotec.2019.05.006

[7] Fakir OE, Wang LL, Balint D, Dear JP, Lin JG, Dean TA (2014) Numerical study of the solution heat solution heat treatment, forming, and in-die quenching (HFQ) process on AA5754. Int J Mach Tools Manu 87: 39-48. https://doi.org/10.1016/j.ijmachtools.2014.07.008

[8] Fan XB, He ZB, Yuan SJ, Lin P (2013) Investigation on strengthening of 6A02 aluminum alloy sheet in hot forming-quenching integrated process with warm forming-dies. Mater Sci Eng A 587: 221-227. https://doi.org/10.1016/j.msea.2013.08.059

[9] Kitayama S, Natsume S, Yamazaki K, Han J, Uchida H (2016) Numerical investigation and optimization of pulsating and variable blank holder force for identification of formability window for deep drawing of cylindrical cup. Int J Adv Manuf Technol 82(1): 583-593. https://doi.org/10.1007/s00170-015-7385-7

[10] Komgrit L, Hamasaki H, Hino R, Yoshida F (2016) Elimination of springback of high-strength steel sheet by using additional bending with counter punch. J Mater

Process Technol 229: 199-206. https://doi.org/10.1016/j.jmatprotec.2015.08.029
[11] Karafillis AP, Boyce MC (1992) Tooling design in sheet metal forming using springback calculations. Int J Mech Sci 34: 113-131. https://doi.org/10.1016/0020-7403(92)90077-T
[12] Su CJ, Zhang K, Lou SM, Xu TT, Wang Q (2017) Effects of variable blank holder forces and a controllable drawbead on the springback of shallow-drawn TA2M titanium alloy boxes. Int J Adv Manuf Technol 93: 1627-1635. https://doi.org/10.1007/s00170-017-0620-7
[13] Zong YY, Liu P, Guo B, Shan DB (2015) Springback evaluation in hot v-bending of Ti-6Al-4V alloy sheets. Int J Adv Manuf Technol 76: 577-585. https://doi.org/10.1007/s00170-014-6190-z
[14] Ma WP, Wang BY, Xiao WC, Yang XM, Kang Y (2019) Springback analysis of 6016 aluminum alloy sheet in hot V-shape stamping. J Cent South Univ 26: 524-535. https://doi.org/10.1007/s11771-019-4024-8
[15] Wang AL, Zhong K, Fakir OE, Liu J, Sun CY, Wang LL, Lin JG, Dean TA (2017) Springback analysis of AA5754 after hot stamping: experiments and FE modelling. Int J Adv Manuf Technol 89: 1339-1352. https://doi.org/10.1007/s00170-016-9166-3
[16] Wang CT, Kinzel G, Altan T (1993) Mathematical modeling of plane-strain bending of sheet and plate. J Mater Process Technol 39: 279-304. https://doi.org/10.1016/0924-0136(93)90164-2
[17] Parsa MH, Ahkami SNA, Pishbin H, Kazami M (2012) Investigating springback phenomena in double curved sheet metals forming. Materials & Design 41: 326-337. https://doi.org/10.1016/j.matdes.2012.05.009
[18] Xue P, Yu TX, Chu E (2001) An energy approach for predicting springback of metal sheets after double-curvature forming, Part II: Unequal double-curvature forming. Int J Mech Sci 43: 1915-1924. https://doi.org/10.1016/S0020-7403(01)00004-2
[19] Leu DK (2019) Relationship between mechanical properties and geometric parameters to limitation condition of springback based on springback-radius concept in V-die bending process. Int J Adv Manuf Technol 101: 913-926. https://doi.org/10.1007/s00170-018-2970-1
[20] Tang BT, Lu XY, Wang ZQ, Zhao Z (2010) Springback investigation of anisotropic aluminum alloy sheet with a mixed hardening rule and Barlat yield criteria in sheet metal forming. Mater Design 31: 2043-2050. https://doi.org/10.1016/j.matdes.2009.10.017
[21] Gau JT, Kinzel GL (2001) A new model for springback prediction in which the Bauschinger effect is considered. Int J Mech Sci 43: 1813-1832. https://doi.org/10.1016/S0020-7403(01)00012-1
[22] Eggertsen PA, Mattiasson K (2009) On the modelling of the bending-unbending behavior for accurate springback predictions. Int J Mech Sci 51: 547-563. https://doi.org/10.1016/j.ijmecsci.2009.05.007
[23] Yoshida F, Uemori T (2002) A model of large-strain cyclic plasticity describing the Bauschinger effect and workhardening stagnation. Int J Plast 18: 661-686. https://doi.org/10.1016/S0749-6419(01)00050-X

[24] Yoshida F, Uemori T (2003) A model of large-strain cyclic plasticity and its application to springback simulation. Int J Mech Sci 45: 1687-1702. https://doi.org/10.1016/j.ijmecsci.2003.10.013
[25] Chatti S, Hermi N (2011) The effect of non-linear recovery on springback prediction. Comput Struct 2011, 89: 1367-1377. https://doi.org/10.1016/j.compstruc.2011.03.010
[26] Zhang DJ, Cui ZS, Ruan XY, Li YQ (2007) An analytical model for predicting springback and side wall curl of sheet after U-bending. Comp Mater Sci 38: 707-715. https://doi.org/10.1016/j.commatsci.2006.05.001
[27] Liu JG, Xue W (2017) Unconstrained bending and springback behaviors of aluminum-polymer sandwich sheets. Int J Adv Manuf Technol 91: 1517-1529. https://doi.org/10.1007/s00170-016-9819-2
[28] Xiao WC, Wang BY, Zheng KL, Zhou J, Lin JG (2018) A study of interfacial heat transfer and its effect on quenching when hot stamping AA7075. Arch Civ Mech Eng 18: 723-730. https://doi.org/10.1016/j.acme.2017.12.001
[29] Zhang ZQ, Zhang XK, He DY (2020) Forming and warm die quenching process for AA7075 aluminum alloy and its application. J. Mater Eng Perform 29:620-625. https://doi.org/10.1007/s11665-019-04545-7
[30] Yang XM, Dang LM, Wang YQ, Zhou J, Wang BY (2020) Springback prediction of TC4 titanium alloy V-bending under hot stamping condition. J Cent South Univ 27: 2578-2591. https://doi.org/10.1007/s11771-020-4483-y
[31] Zhu SQ, Yang W, Jia CL, Wang DG, Liu G, Shi JT, Yuan N, Jin ZL (2017) Research on stress relaxation behavior of TA15 titanium alloy. J Plasticity Engineering 24: 178-182. 10.3969/j.issn.1007-2012.2017.04.029

Figures

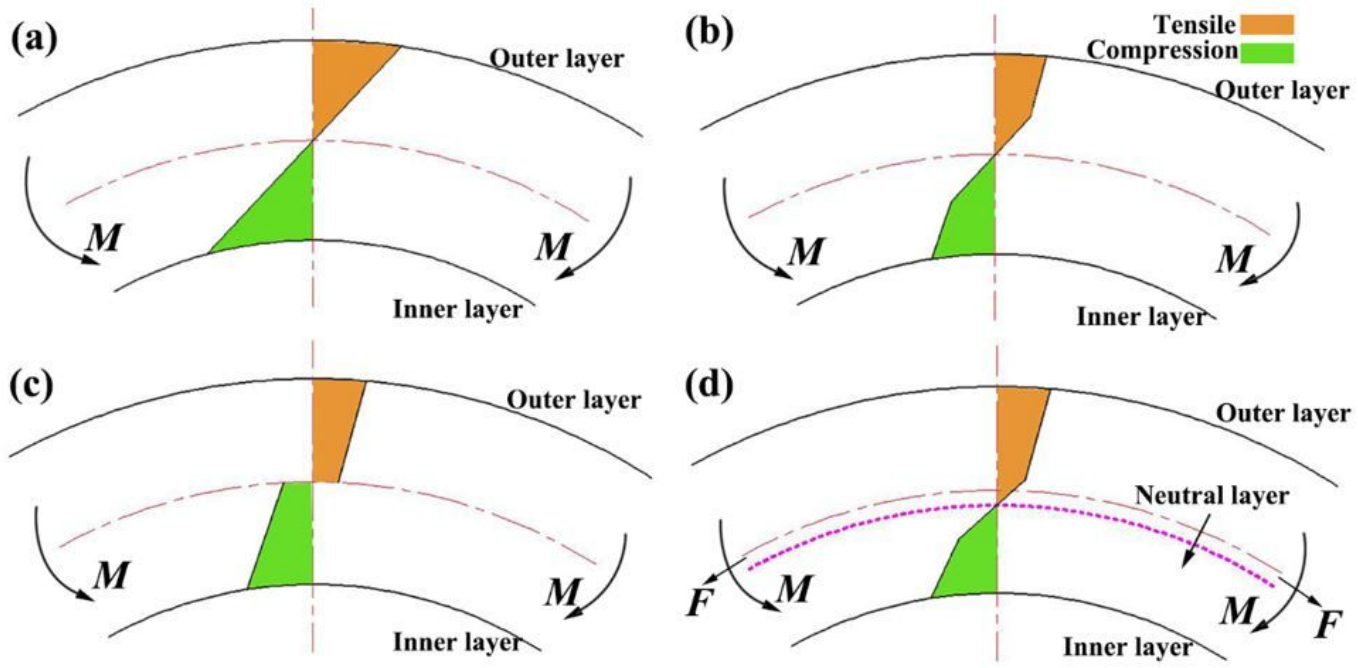

Figure 1

Transverse stress distribution of stretch bending of profile (a) elastic deformation, (b) elastoplastic deformation, (c) pure plastic deformation, and (d) neutral layer transferring

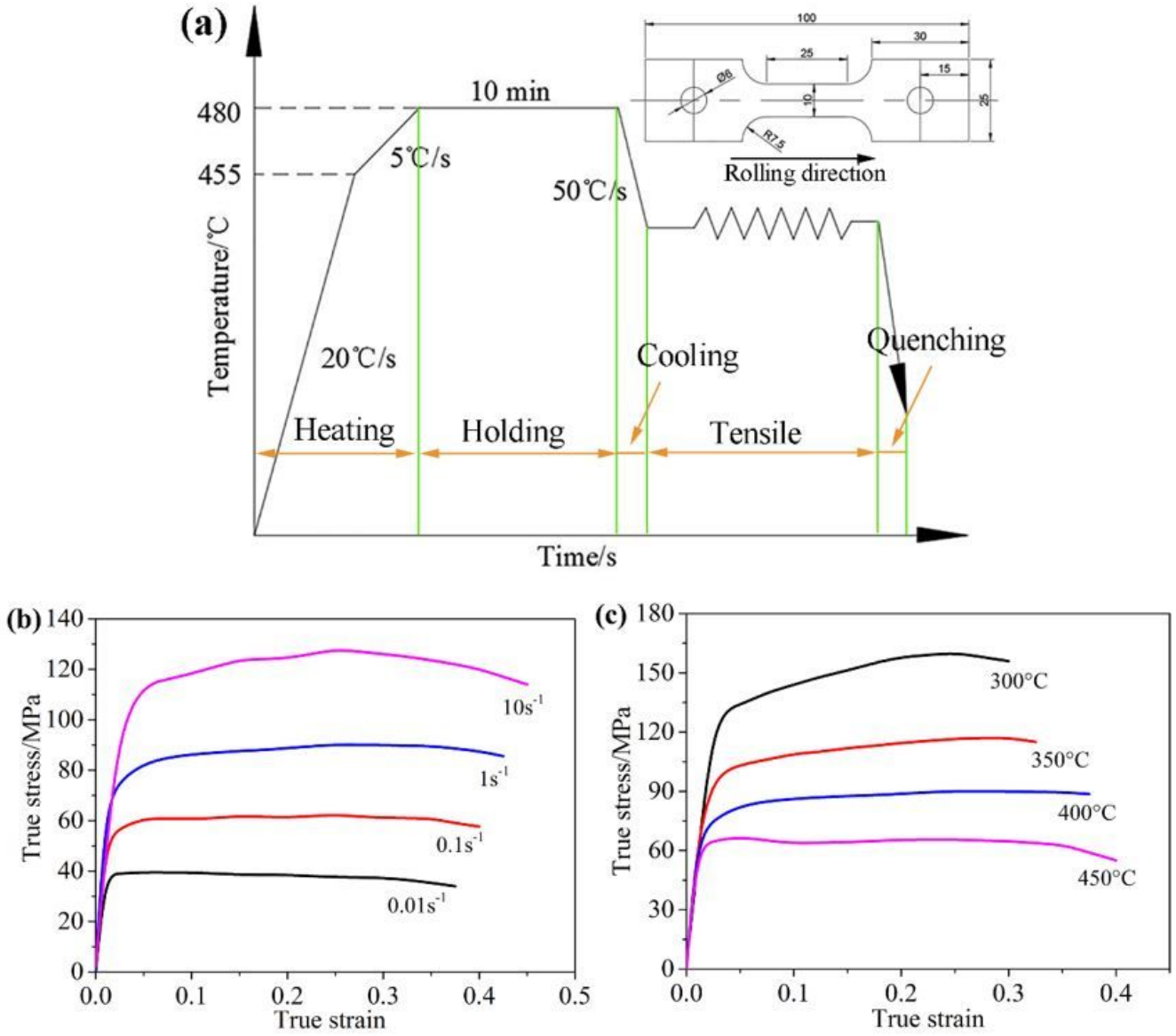

Figure 2

Temperature history of thermal simulation experiments and the obtained true strain-stress curves: (a) temperature history, (b) at deformation temperature of 400 °C, and (c) at strain rate of 1 s-1

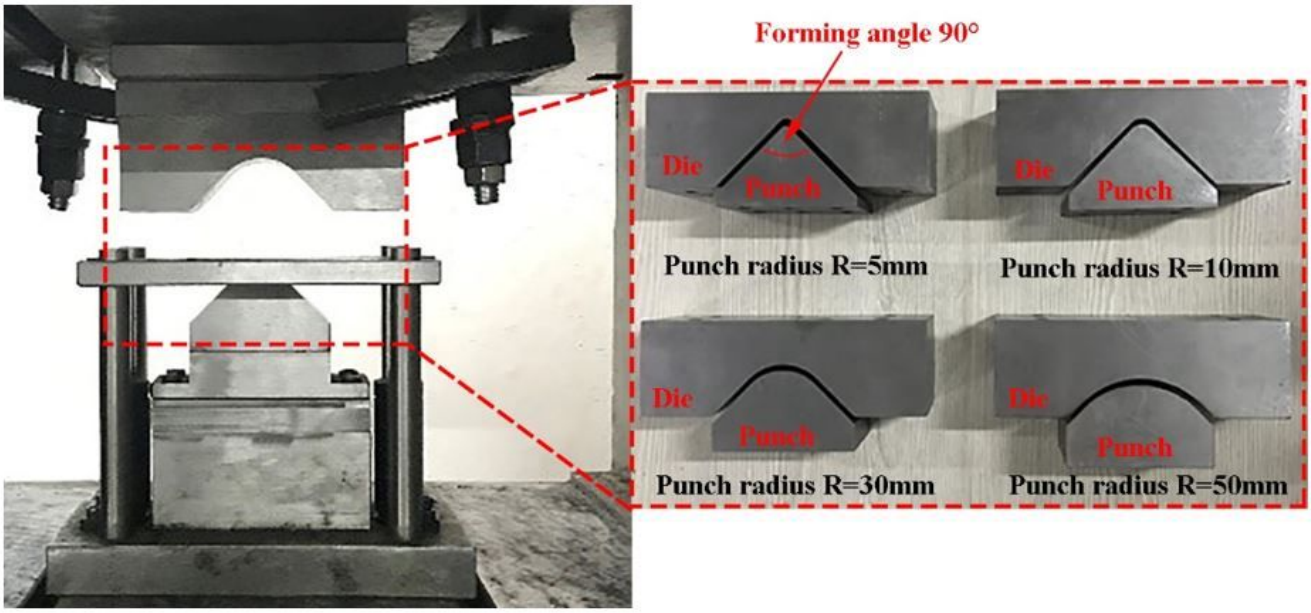

Figure 3

The V-shaped stamping tools

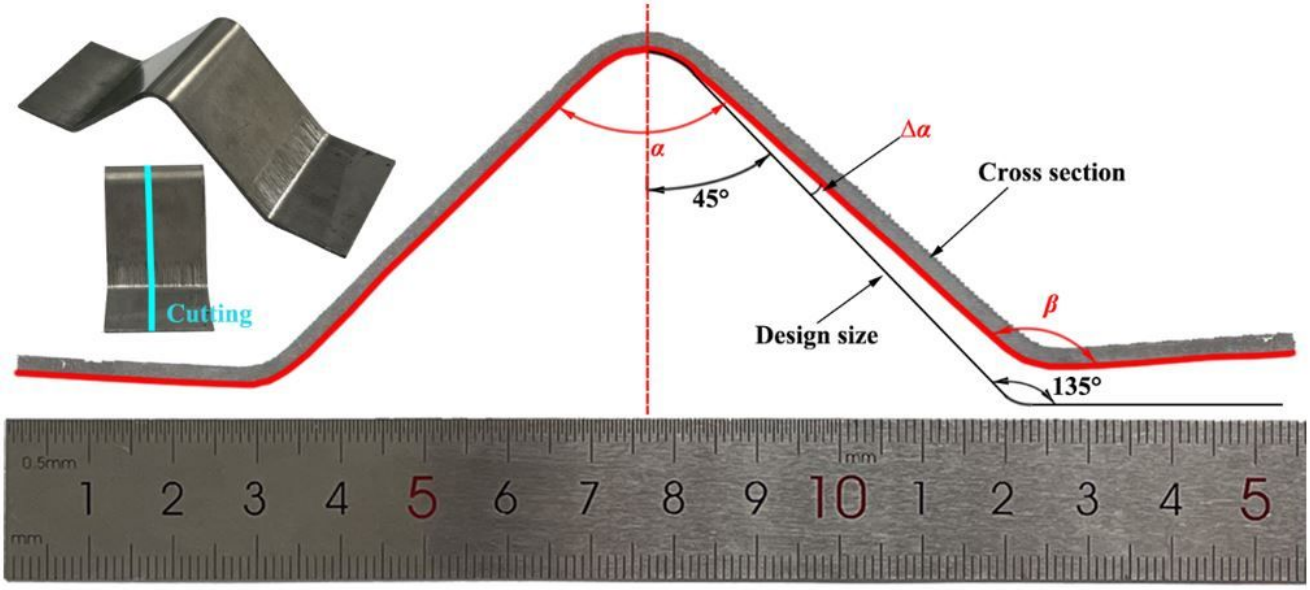

Figure 4

The measurement of the springback angles

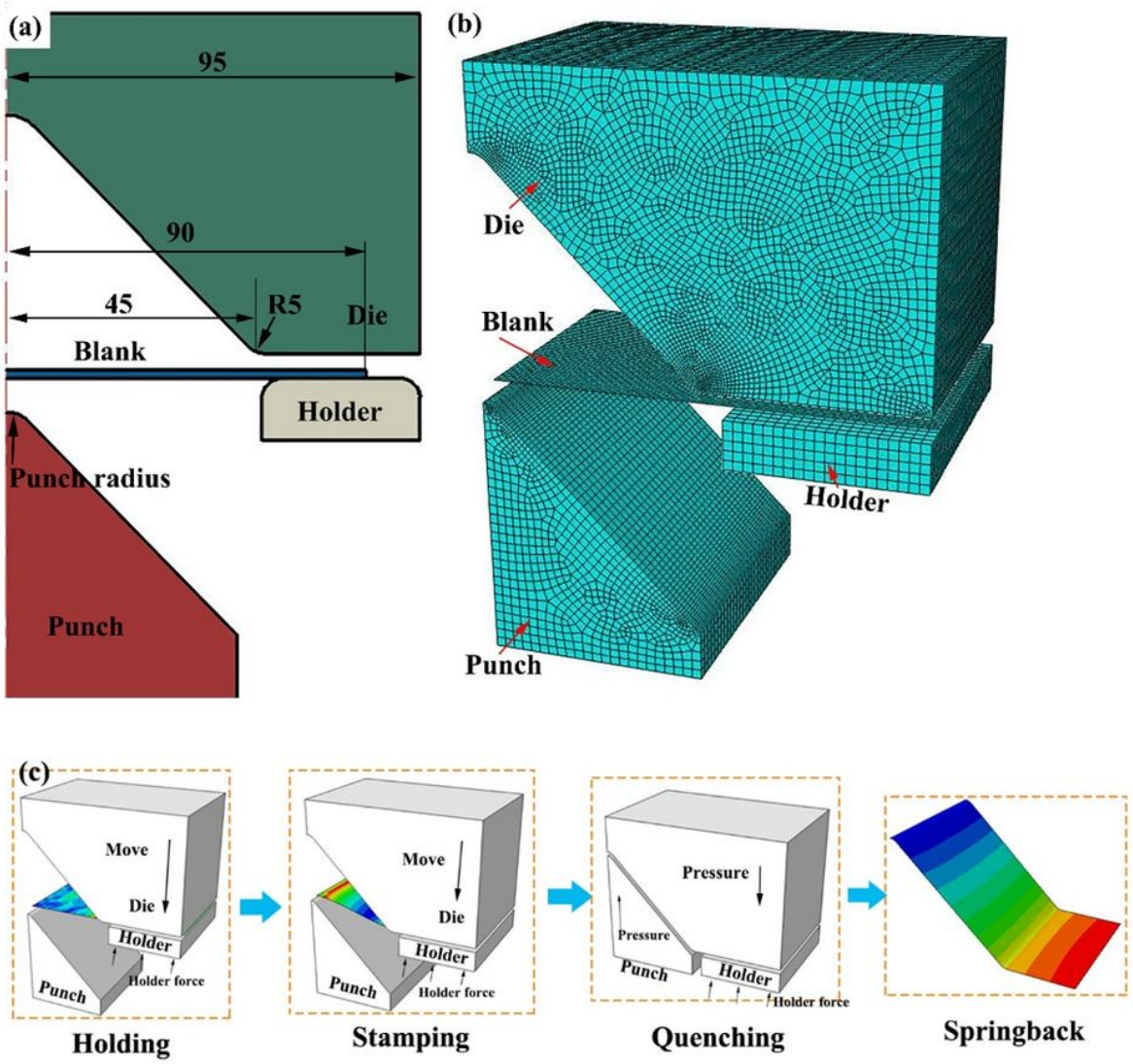

Figure 5

The V-shaped FE model (a) the size of the FE model, (b) the FE model, and (c) the simulation procedure

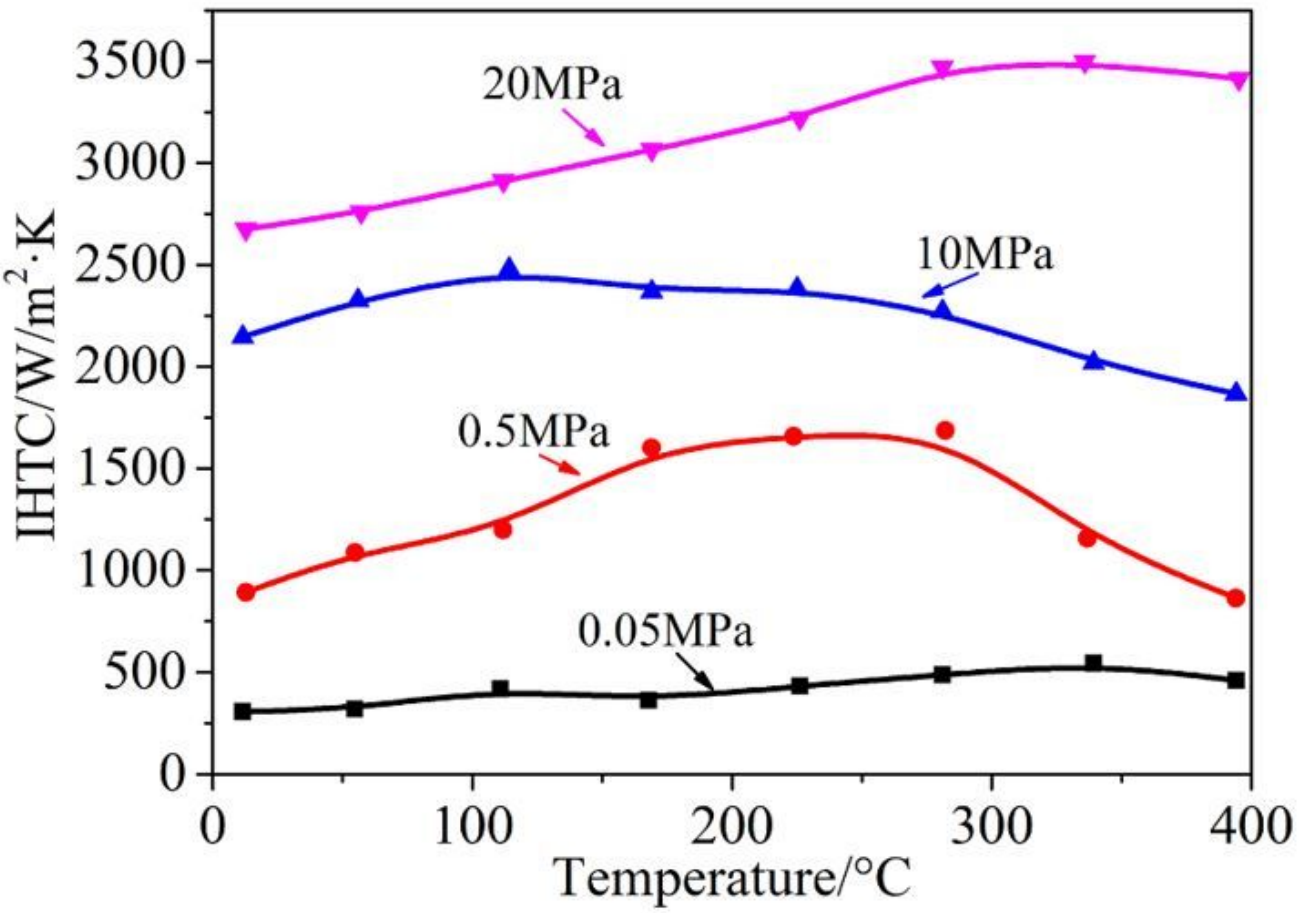

Figure 6

Interfacial heat transfer coefficient of the AA7075 and H13 steel contact pair

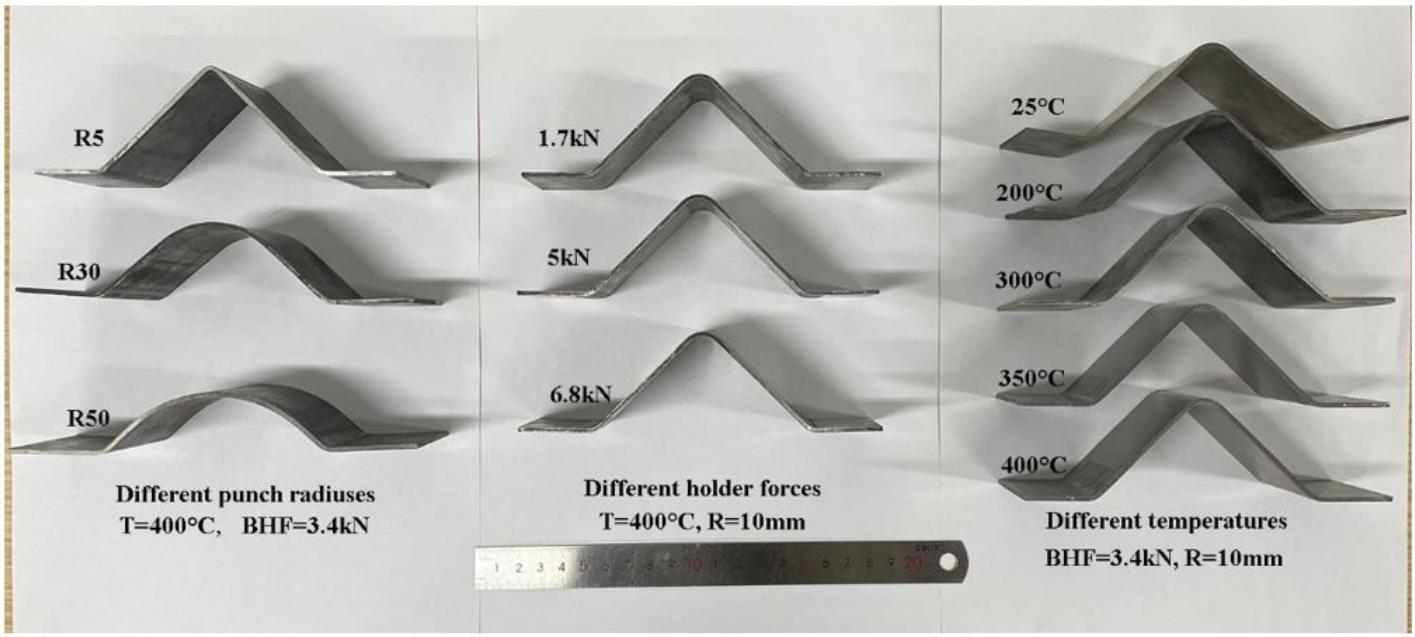

Figure 7

The formed parts at different parameters

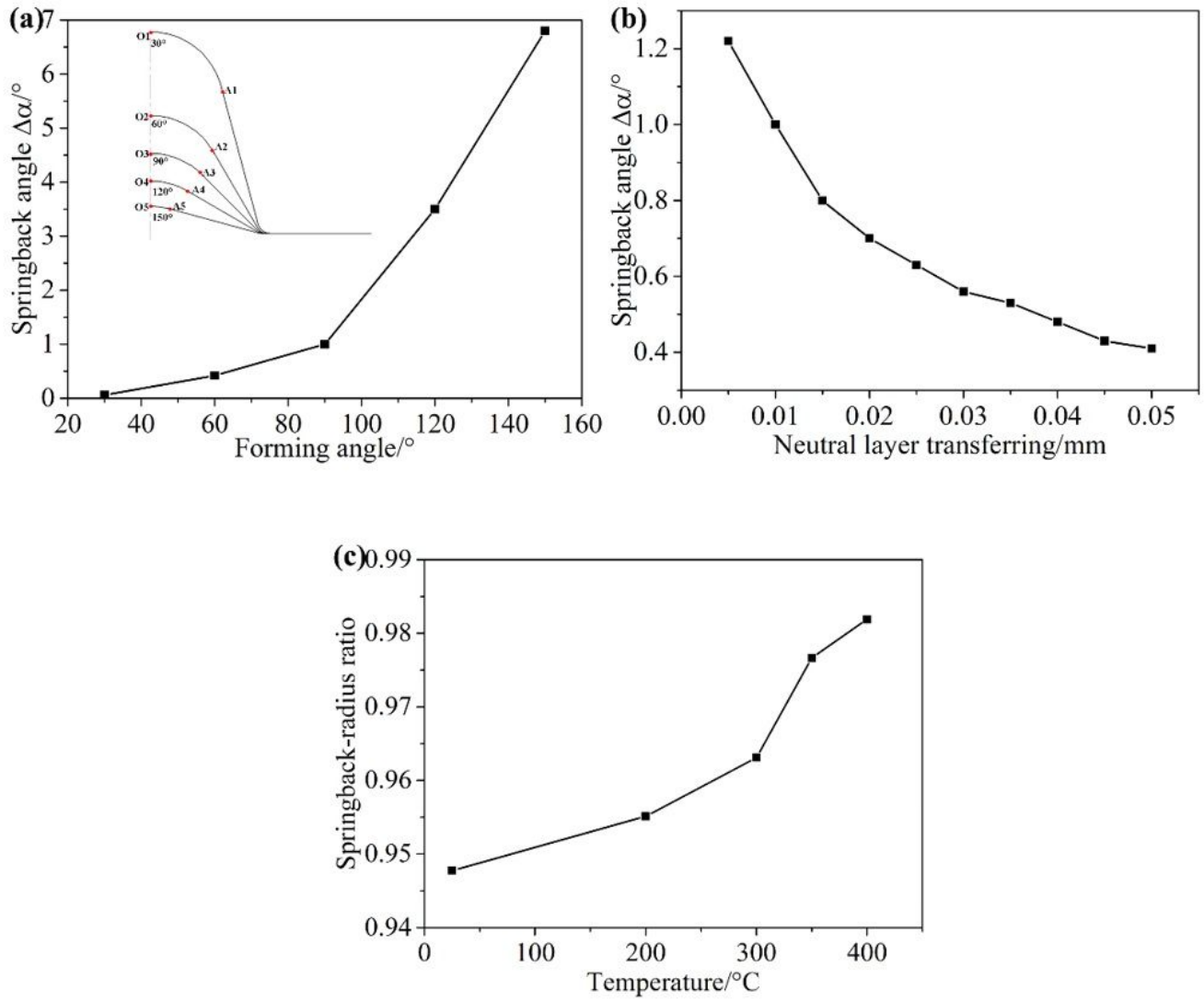

Figure 8

The effect of process parameter on springback (a) forming angle, (b) neutral layer transferring, and (c) the change of springback-radius ratio for angle β

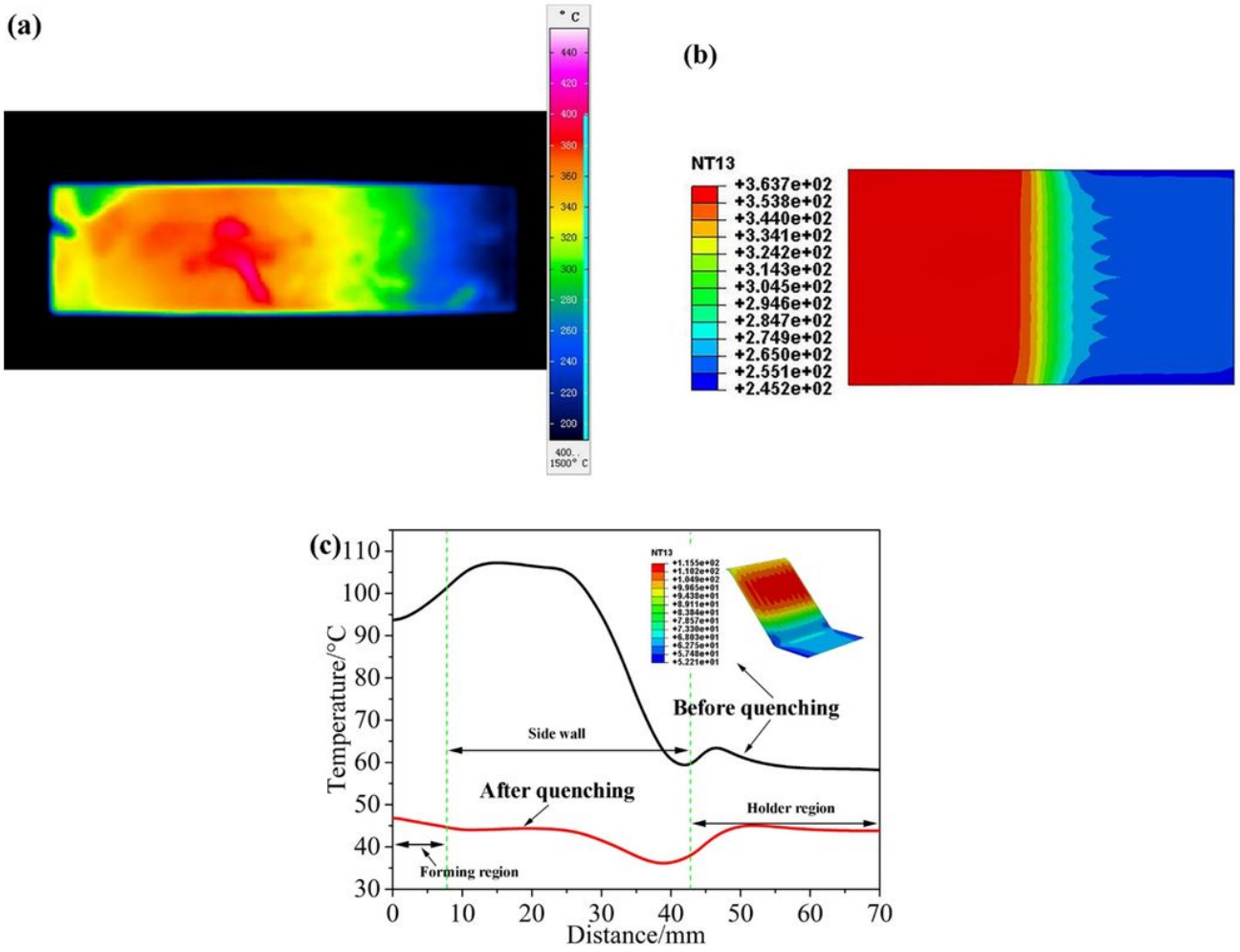

Figure 9

The temperature distribution of sheet (a) experimental result after holding, (b) simulation result after holding, and (c) temperature distribution variation after stamping

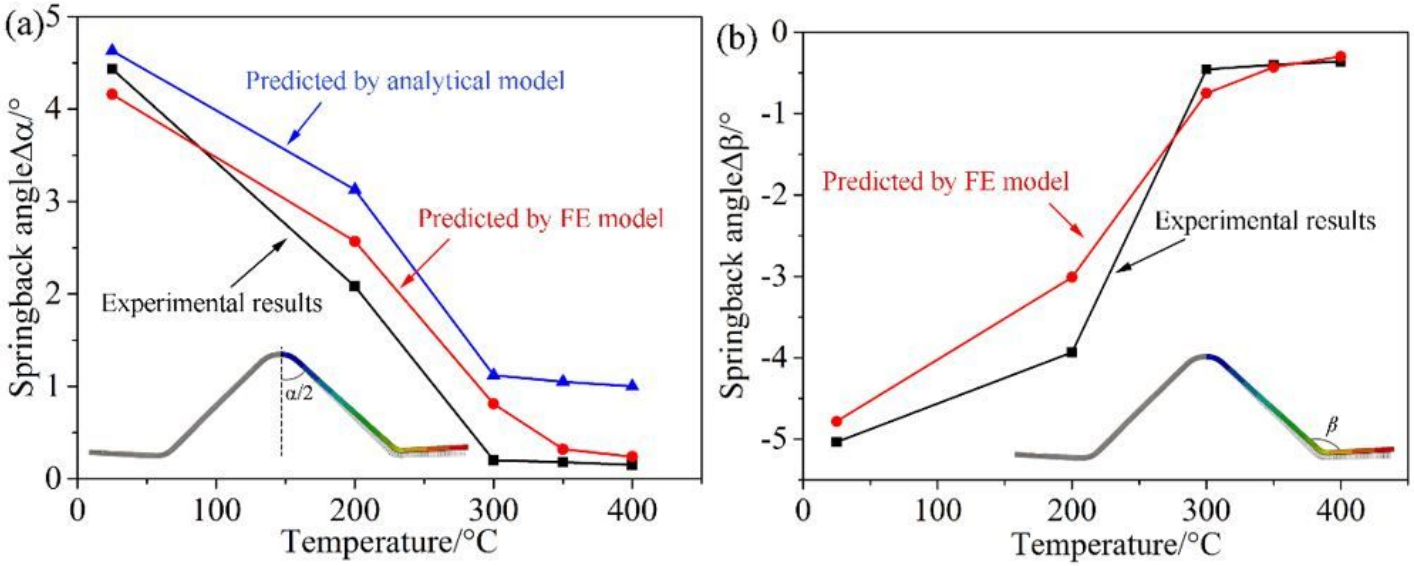

Figure 10

The change of springback angles (a) the change of springback angle Δα, and (b) the change of springback angle Δβ

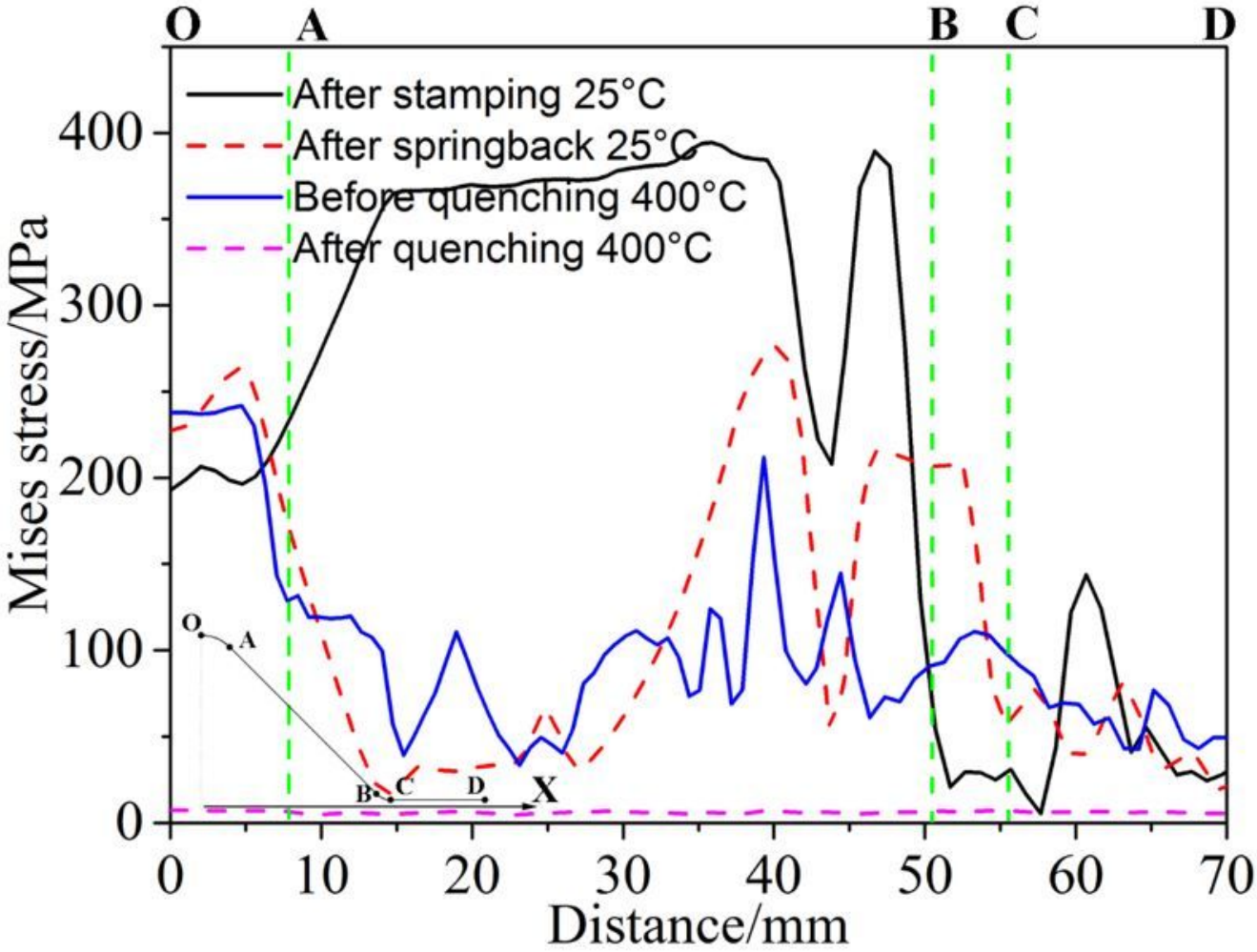

Figure 11

The distribution of Mises stress along a section at different process stages and temperatures

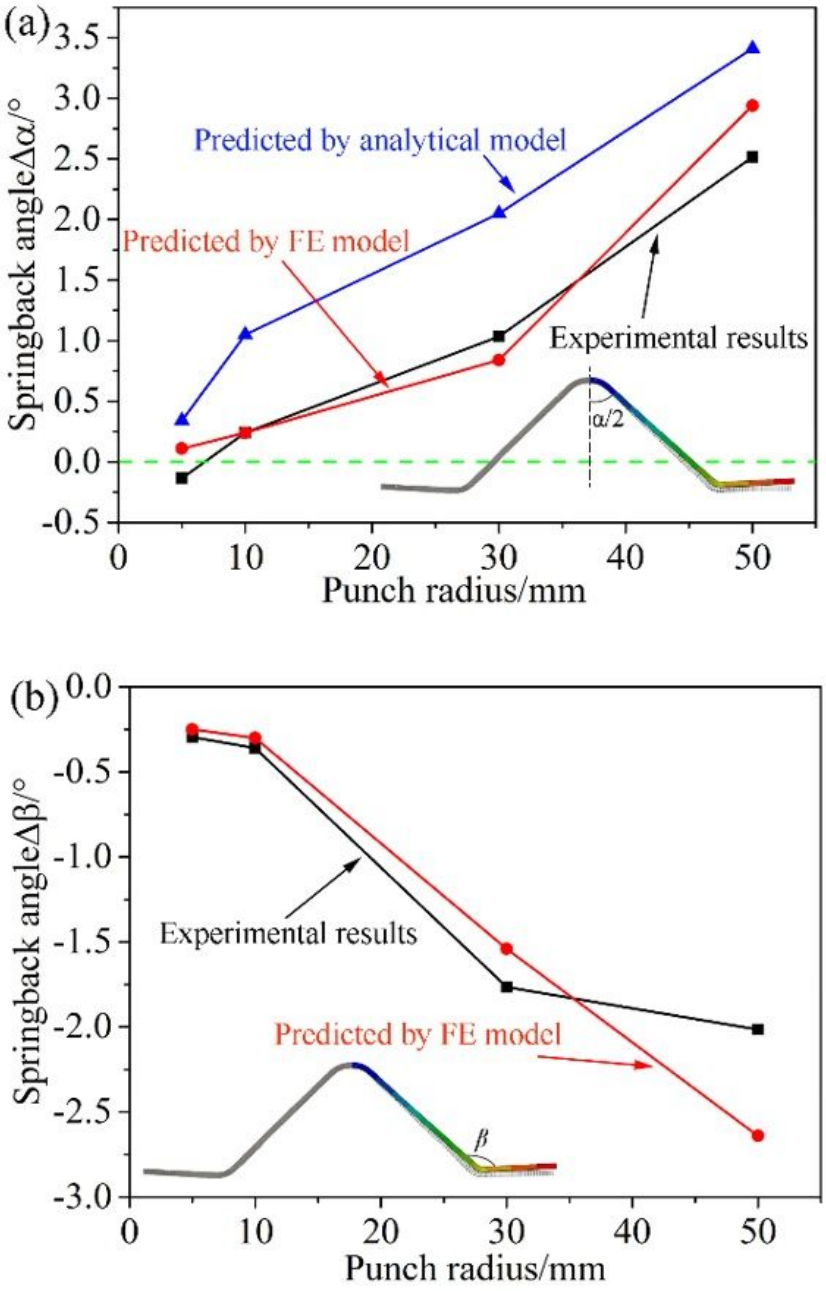

Figure 12

Influence of punch radius on springback angles (a) the change of springback angle Δα, and (b) the change of springback angle Δβ

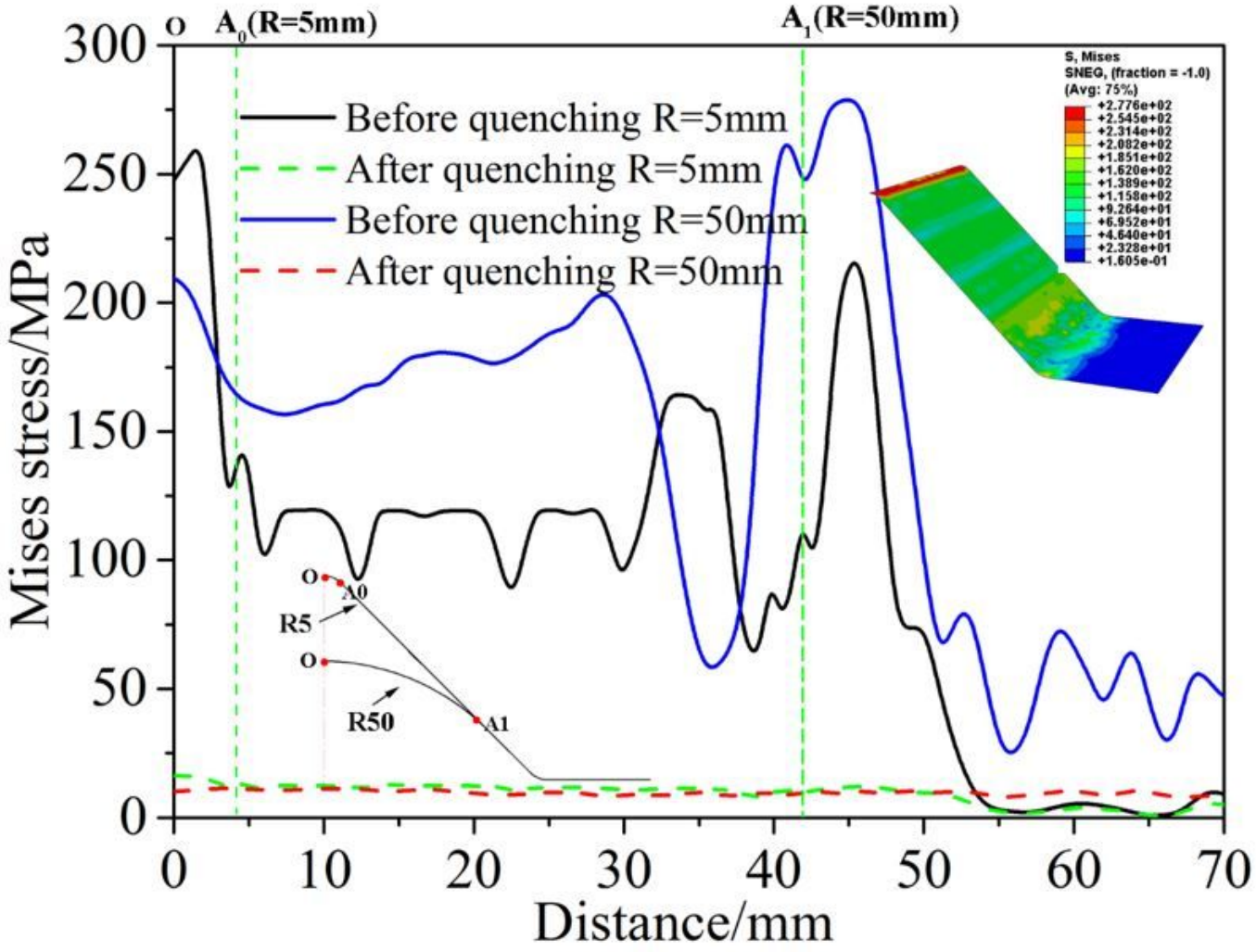

Figure 13

The distribution of Mises stress along a section at different process stages and punch radiuses

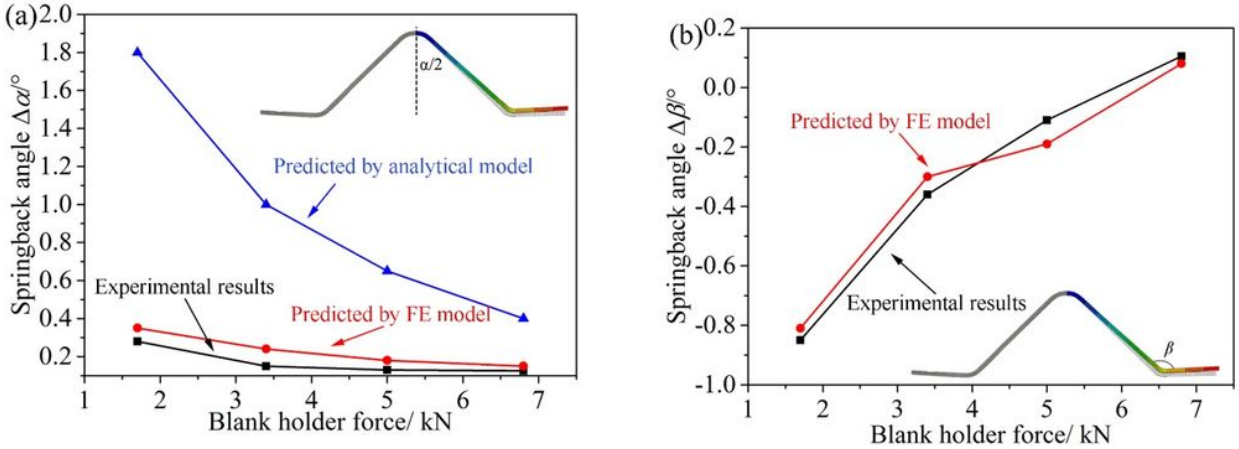

Figure 14

Influence of blank holder force on springback angles (a) the change of springback angle Δα, and (b) the change of springback angle Δβ

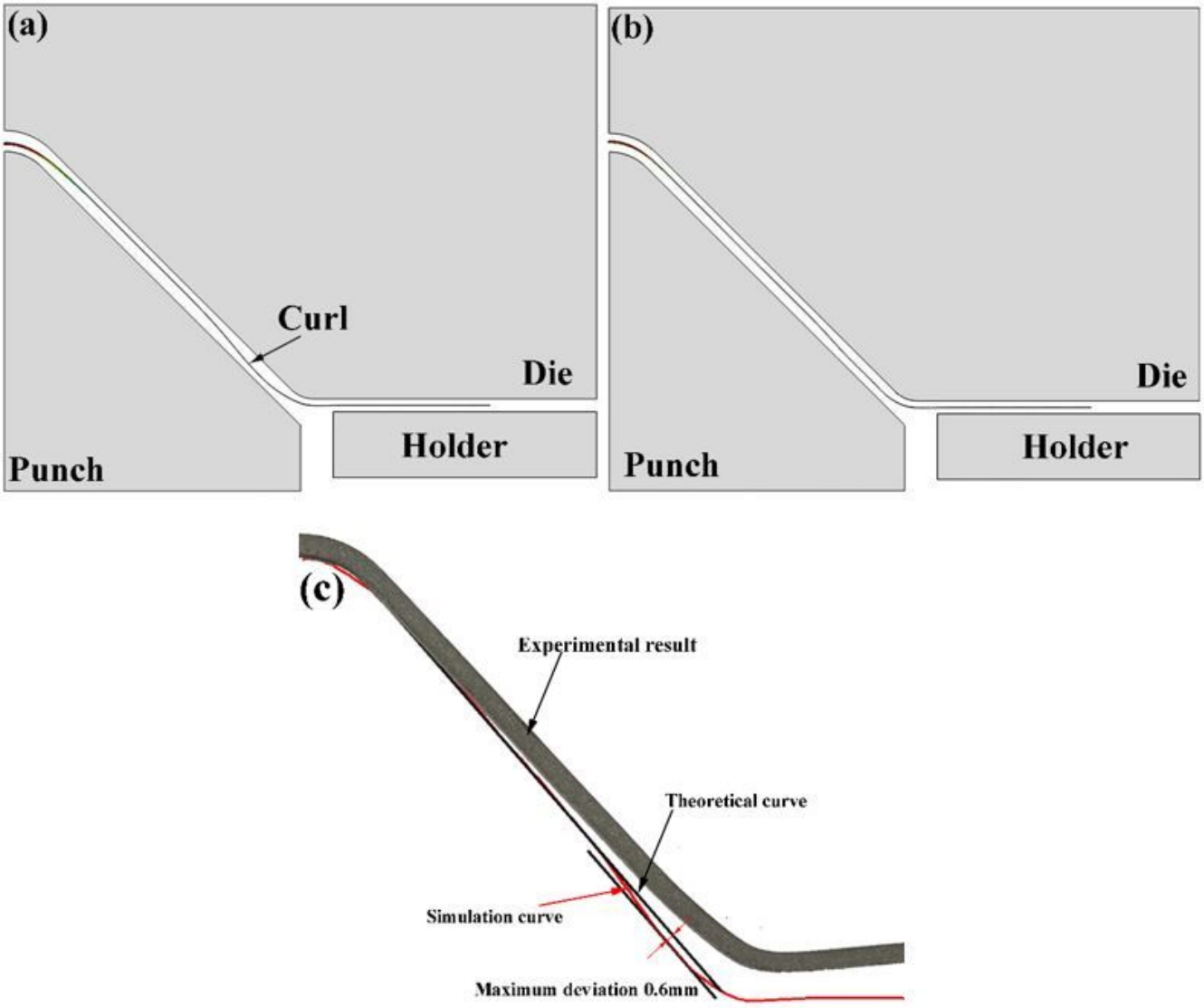

Figure 15

The curl of side wall at different blank holder forces (a) blank holder force 1.7 kN, (b) blank holder force 6.8 kN, and (c) deviation causing by curl